IMMUNOLOGY

Lupus susceptibility gene *Pbx1* controls the development, stability, and function of regulatory T cells via *Rtkn2* expression

Seung-Chul Choi[1], Yuk Pheel Park[1], Tracoyia Roach[1], Damian Jimenez[1], Amanda Fisher[1], Mojgan Zadeh[1], Longhuan Ma[1], Eric S. Sobel[2], Yong Ge[1], Mansour Mohamadzadeh[1], Laurence Morel[1]*

The maintenance of regulatory T (T_{reg}) cells critically prevents autoimmunity. Pre–B cell leukemia transcription factor 1 (*Pbx1*) variants are associated with lupus susceptibility, particularly through the expression of a dominant negative isoform *Pbx1-d* in $CD4^+$ T cells. *Pbx1-d* overexpression impaired T_{reg} cell homeostasis and promoted inflammatory $CD4^+$ T cells. Here, we showed a high expression of *Pbx1* in human and murine T_{reg} cells, which is decreased in lupus patients and mice. *Pbx1* deficiency or *Pbx1-d* overexpression reduced the number, stability, and suppressive activity of T_{reg} cells, which increased murine responses to immunization and autoimmune induction. Mechanistically, *Pbx1* deficiency altered the expression of genes implicated in cell cycle and apoptosis in T_{reg} cells. Intriguingly, *Rtkn2*, a Rho-GTPase previously associated with T_{reg} homeostasis, was directly transactivated by Pbx1. Our results suggest that the maintenance of T_{reg} cell homeostasis and stability by *Pbx1* through cell cycle progression prevent the expansion of inflammatory T cells that otherwise exacerbates lupus progression in the hosts.

INTRODUCTION

$FOXP3^+$ regulatory T (T_{reg}) cells are critically involved in the maintenance of immune homeostasis (*1*). Reducing the number and function of T_{reg} cells impairs immune tolerance, leading to abnormal immune responses to self-antigens, thus resulting in inflammation and autoimmune diseases (*2*). T_{reg} cells develop from $CD4^+$ autoreactive thymocytes that are activated via CD28/Lck signaling, the IL-2–CD25–Stat5 axis, and T cell receptor (TCR)–major histocompatibility complex (MHC)–self-peptide complexes (*3*), which induce a cell-specific hypomethylation of the *Foxp3* locus. This induces the expression of *Foxp3* and that of other genes defining T_{reg} cell lineage identity and suppressive function (*4*, *5*). Systemic lupus erythematosus (SLE) is an autoimmune disease in which T_{reg} dysfunctions have been documented in patients with either decreased numbers (*6*), suppressive functions, or both (*7*), as well as in mouse models of the disease. Moreover, the T_{reg}-specific deletion or overexpression of several genes that impair T_{reg} functions resulted in lupus-like phenotypes in murine models (*8*).

A large number of genetic polymorphisms have been associated with SLE susceptibility (*9*). In parallel, we have identified lupus susceptible loci in the NZM2410 mouse model (*10*). Among them, *Sle1a1* regulates the effector fate and function of $CD4^+$ T cells, and it contains only one protein-coding gene, *Pbx1* (*11*–*13*). Pbx1 is a transcription factor that regulates chromatin access of multimeric complexes that include Hox factors, Meis and Prep-1, to regulate coactivator or repressor access (*14*, *15*). *Pbx1* is necessary for the maintenance of hematopoietic stem cells (*16*, *17*) and for the development of B cells from common lymphoid progenitors (CLPs) (*18*). A 3′ untranslated region single-nucleotide polymorphism is associated with decreased PBX1 expression in peripheral blood mononuclear cells (PBMCs) as well as with SLE susceptibility (*19*). A reduced expression of *PBX1* in the B cells of patients with SLE correlated with disease activity, and a B cell–specific deletion of *Pbx1* resulted in enhanced responses to immunization as well as to the chronic graft versus host disease (cGVHD)–induced model of lupus (*19*).

The Prep/Pbx1 complex regulates some developmental stages in double-negative T cells in the thymus (*20*). Furthermore, *Pbx1* deficiency reduced the number of T cells produced from fetal liver chimeras (*18*). The association of *Pbx1* with lupus in T cells was established through *Pbx1-d*, a splice isoform lacking the DNA binding and Hox-binding domains, as compared to *Pbx1-b*, the common isoform in lymphocytes. *Pbx1-d* expression was higher in the $CD4^+$ T cells from B6.*Sle1a* and NZM2410 mice as well as from patients with SLE, as compared to healthy controls (HCs) (*13*). Pbx1-d functions as a dominant negative (DN) allele (*21*), and accordingly, its expression impaired the immunosuppressive function of mesenchymal stem cells (*22*). *Pbx1-d* expression was also associated with abnormal responses to transforming growth factor–β (TGF-β) and retinoic acid in murine and human T cells (*23*), suggesting that it could impair T_{reg} cell homeostasis. Accordingly, *Pbx1-d* transgenic (Tg) expression in T cells reduced the number of T_{reg} cells and their in vitro polarization, as well as increased the number of inflammatory $CD4^+$ T cells (*24*), which reproduced the phenotypes of B6.*Sle1a* mice (*11*, *13*).

Here, we showed that T_{reg} cells are the $CD4^+$ T cell subset in which *PBX1* is expressed at the highest level, with a reduced expression in both lupus-prone mice and patients with SLE. T_{reg} cell–specific *Pbx1* deletion or T_{reg} cell–specific *Pbx1-d* sole expression reduced the number of peripheral T_{reg} cells and their suppressive activity with a concomitant accumulation of inflammatory effector $CD4^+$ T cells. This resulted in an increased humoral response to protein immunization as well as increased T cell activation and autoantibody response to induced lupus in mice. Fate-mapping reporter mice showed that an increased frequency of *Pbx1-d* Tg T_{reg} cells lost *Foxp3* expression and differentiated into T follicular helper cells (T_{FH}). Mechanistically, *Pbx1* regulates the expression of genes in the cell cycle, apoptosis, and migration pathways in T_{reg} cells. Among

[1]Department of Microbiology, Immunology, and Molecular Genetics, University of Texas Health San Antonio, TX 78229-3900, USA. [2]Department of Medicine, University of Florida, Gainesville, FL 32610, USA.
*Corresponding author. Email: morel@uthscsa.edu

these genes, Pbx1 directly transactivates the expression of *Rtkn2*, a Rho protein that regulates cell cycle and apoptosis (*25*). Accordingly, *Pbx1*-deficient T_{reg} cells as well as Jurkat T cells overexpressing *PBX1-D* showed a reduced proliferation. These results suggest that Pbx1 regulates T_{reg} cell proliferation, stability, and suppressive functions, which are altered by the expression of the *Pbx1-d* lupus–associated isoform.

RESULTS

PBX1 is preferentially expressed in T_{reg} cells among $CD4^+$ T cells

PBX1 expression is lower in the PBMCs from patients with SLE and in the B cells from patients and lupus-prone mice than in the corresponding HCs (*19*). *PBX1* expression was however not assessed in $CD4^+$ T cells in this study. Since the overexpression of the lupus-associated *Pbx1-d* isoform in murine T cells impaired T_{reg} cell homeostasis (*24*), we hypothesized that Pbx1 may intrinsically regulate T_{reg} cells. We compared *Pbx1* expression between T_{reg} and non-T_{reg} T cells isolated from three lupus-prone mouse strains, B6.*Sle1.Sle2.Sle3* (TC), (NZB x NZW)F1 (BWF1), and BXSB.Yaa, which all share the same susceptibility locus on chromosome 1 containing *Pbx1* (*26*), as well as B6 controls. The three lupus strains expressed a similar level of *Pbx1* in T_{reg} cells, which was lower compared to B6 (fig. S1A and Fig. 1A). There was however no difference between strains for non-T_{reg} T cells (fig. S1B and Fig. 1B). Furthermore, T_{reg} cells expressed, on average, seven times more *Pbx1* than their non-T_{reg} T cells counterparts, regardless of their strain of origin (Fig. 1C and fig. S1, C and D). Similar results were obtained for the expression of *Pbx1-d* (fig. S1, E and F). Both T_{reg} and non-T_{reg} cells from patients with SLE expressed less *PBX1* than HCs (Fig. 1, D and E), but as in mice, human T_{reg} cells expressed higher amount of *PBX1* (17 times higher on average) than their non-T_{reg} counterparts (Fig. 1F). *PBX1-D* expression was higher in the T_{reg} cells from patients with SLE (Fig. 1G), with no difference in non-T_{reg} T cells (Fig. 1H), resulting in a *PBX1-D* expression, on average, 250-fold higher in T_{reg} versus non-T_{reg} T cells (Fig. 1I). We confirmed that the relative expression of *PBX1-D* was higher in SLE $CD4^+$ T cells (Fig. 1, J and K), which resulted in SLE T_{reg} expressing the highest levels of *PBX1-D* (Fig. 1L). Overall, T_{reg} cells are the $CD4^+$ T cell subset in which *PBX1* expression is the highest, with a shift in the relative expression of *PBX1-D* over *PBX1*, suggesting that *PBX1* may play a role in T_{reg} cell homeostasis.

Pbx1 expression regulates the maintenance of peripheral T_{reg} cells

To explore the role of Pbx1 in T_{reg} cells, we generated B6.$Pbx1^{f/f}$.$Foxp3^{YFP\text{-}Cre}$ mice (referred thereafter as KO) with a T_{reg}-specific *Pbx1* deletion (fig. S1, G and H). In addition, KO mice were bred with *Cd4-Pbx1-d* Tg mice that express *Pbx1-d* driven by the *Cd4* promoter (*24*), to produce B6.$Pbx1^{f/f}$.$Foxp3^{YFP\text{-}Cre}$.*Cd4-Pbx1-d* Tg (KO-Tg) mice that have T_{reg} cells expressing solely the *Pbx1-d* isoform. B6.$Foxp3^{YFP\text{-}Cre}$.*Cd4-Pbx1-d* Tg (Tg) mice were used as *Pbx1-d* Tg mice to control for the expression of $Foxp3^{YFP\text{-}Cre}$. Young KO and Tg mice showed a decreased frequency of total splenic T_{reg} cells, whereas it was similar between KO-Tg and wild-type (WT) mice (Fig. 2, A and B). The frequency of thymic-derived NRP-1^+ natural T_{reg} (nT_{reg}) cells was similar between strains. However, the frequency of NRP-1–negative peripherally induced T_{reg} (iT_{reg}) cells was decreased in KO, KO-Tg, and Tg mice. Accordingly, T_{reg} cells negative for Helios expression, a

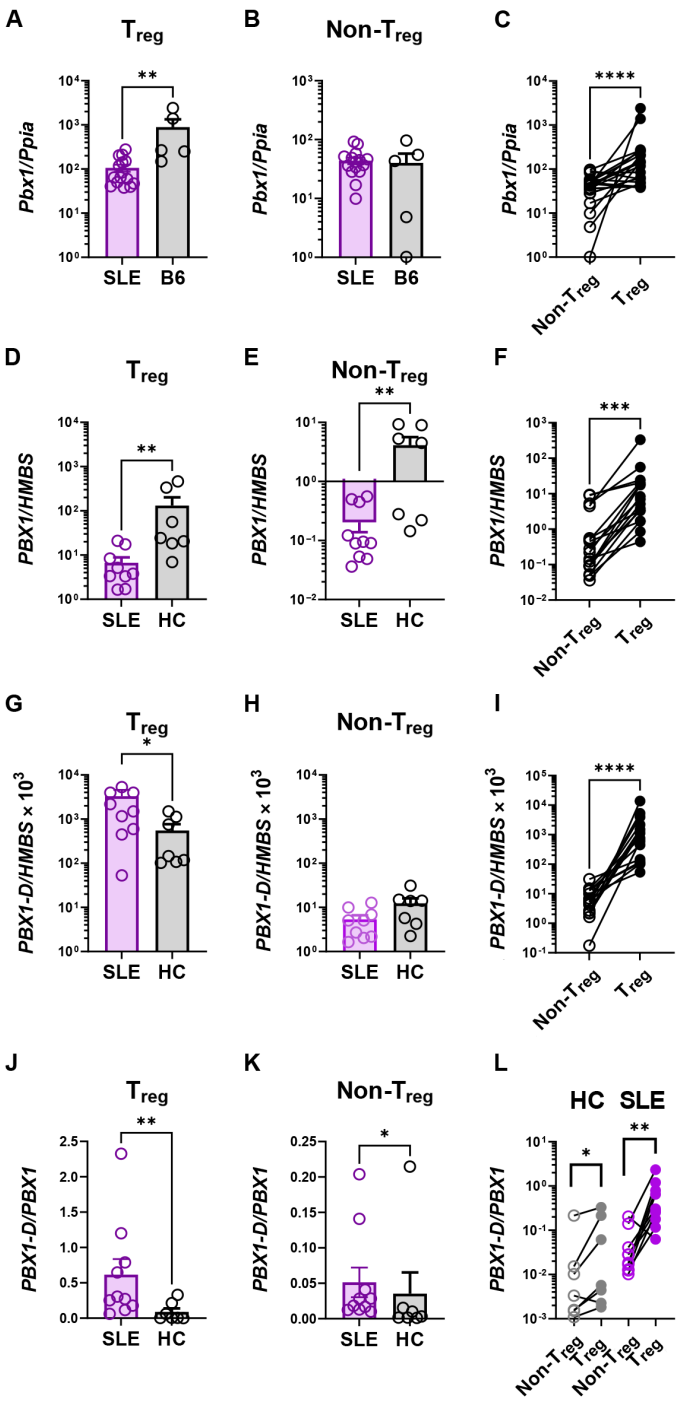

Fig. 1. *PBX1* is preferentially expressed in T_{reg} cells. (**A** to **C**) *Pbx1* expression in murine T_{reg} (A) and non-T_{reg} T (B) cells from B6 and the combination of three lupus-prone strains (SLE: TC, BWF1, and BXSB.Yaa). (C) Paired analysis between T_{reg} and non-T_{reg} cells for all strains combined ($N = 5$ per strain). (**D** to **I**) *PBX1* (D to F) and *PBX1-D* [(G) to (I)] expression in human T_{reg} [(D) and (G)] and non-T_{reg} (E and H) T cells from patients with SLE ($N = 10$) and HCs ($N = 7$). (F) and (I) Paired analysis between T_{reg} and non-T_{reg} cells for all human samples combined. (**J** to **L**) *PBX1-D/PBX1* ratios corresponding to the human T cells shown in (D) to (I). Mean + SEM compared with Mann-Whitney tests or paired t tests. $^*P < 0.05$, $^{**}P < 0.01$, $^{***}P < 0.001$, and $^{****}P < 0.0001$.

marker of thymic origin (*27*), represented a smaller proportion of total T_{reg} cells in these *Pbx1*-altered strains (fig. S1I). The frequency of iT_{reg} cells and Helios-negative T_{reg} cells was also reduced in old KO and KO-Tg mice, although their frequency of nT_{reg} cells was increased (fig. S1, J to L). Since a large number of iT_{reg} cells are generated in the gut in response to food antigens as well as the microbiota (*28*), we investigated whether *Pbx1* deficiency affected T_{reg} cells in the gut. KO mice presented an altered frequency of non-T_{reg} T cells with a higher frequency in the colon and a lower frequency in the small intestine (fig. S2A). There was no difference, however, for the ratio of iT_{reg}/nT_{reg} or the frequency of total, nT_{reg}, or iT_{reg} cells (fig. S2, B to E). As in the spleen (Fig. 2B and fig, S1, K and L), the mesenteric lymph node (mLN) of KO mice presented a lower iT_{reg}/nT_{reg} ratio (fig. S2B). Last, the KO Tr_{eg} cells expressed a lower level of FOXP3 in the colon and the mLN than WT T_{reg} cells (fig. S2, F to H).

Pbx1 deficiency or *Pbx1-d* expression in T_{reg} cells had minimal effects on thymic nT_{reg} cells, with a small decreased frequency in young KO mice (fig. S3A) and a small increased frequency in old KO and KO-Tg mice (fig. S3C) but no difference in numbers at either age. The frequency and number of thymic iT_{reg} cells were increased in young KO and KO-Tg mice (fig. S3B), potentially due to an increased trafficking. The frequency and number of thymic iT_{reg} cells were however decreased in old KO and KO-Tg mice as observed in the spleen (figs. S1I and S3D). We next assessed whether *Pbx1* deficiency in total T cells would impair T_{reg} cell differentiation. At steady state, the frequency of splenic T_{reg} cells was higher in $Pbx1^{CD4\text{-}KO}$ mice, but their number was similar to controls (fig. S3E). No difference was observed for thymic total and nT_{reg} cells, but the number of thymic iT_{reg} cells was reduced in $Pbx1^{CD4\text{-}KO}$ mice (fig. S3F). Last, in vitro T_{reg} polarization was not impaired in $CD4^+$ T cells in which *Pbx1* was deleted after (fig. S3G) or before [fig. S3H and (*29*)] *Foxp3* expression, indicating that *Pbx1* expression is not required for T_{reg} differentiation. Pbx1-d expression, however, impaired iT_{reg} polarization (*24*, *29*), and the reason behind the difference between *Pbx1* KO and *Pbx1-d* Tg in vitro is unclear. Overall, these results suggested that *Pbx1* deficiency or the expression of the *Pbx1-d* DN isoform impaired peripheral T_{reg} cell maintenance.

Pbx1 deficiency impairs T_{reg} cell functions

We next determined the protein expression of markers associated with T_{reg} function in older mice with defective *Pbx1* expression in their T_{reg} cells. The expression of FOXP3, the master transcription factor for T_{reg} cells, was reduced in total T_{reg} cells and nT_{reg} cells in KO and KO-Tg and, to a lesser extent, in Tg mice (fig. S4A). *Pbx1* deficiency or *Pbx1-d* sole expression in T_{reg} cells also altered the expression of other markers in T_{reg} cells. The expression of CD25, the high affinity interleukin-2 (IL-2) receptor α subunit, as well as the IL-2Rβ subunit, was reduced by *Pbx1* deficiency and, to a greater extent, by *Pbx1-d* sole expression (fig. S4, B and C). The expression of Glucocorticoid-Induced TNFR-Related (GITR), an activation marker highly expressed on T_{reg} cells, but whose activation has been linked to a decreased suppressive activity (*30*), was increased in nT_{reg} and non-T_{reg} cells from KO and KO-Tg mice (fig. S4D). Both nT_{reg} and iT_{reg} cells also showed an increased expression of CD39 and CD73 (fig. S4, E and F), two ectoenzymes that degrade adenosine nucleosides that are expressed at high levels by T_{reg} cells and linked to their suppressive activity (*31*). On the other hand, nT_{reg} cells from KO, KO-Tg, and Tg mice showed a reduced level of the transcription factor RAR-related orphan receptor gamma (RORγt) (fig. S4G), which is expressed by a T_{reg} subset with enhanced effector functions in which it stabilizes *Foxp3* expression (*32*). The expression of B-cell lymphoma 2 (BCL-2), which is critical for T_{reg} survival (*33*), was also reduced in nT_{reg} and iT_{reg} cells with defective *Pbx1* expression (fig. S4H). Inducible T Cell Costimulator (ICOS) expression was increased in KO and KO-Tg nT_{reg} and iT_{reg} cells (fig. S4J). Although ICOS expression on T_{reg} cells has been associated with enhanced suppressive functions, an expanded population of $ICOS^+$ T_{reg} cells has been reported in patients with SLE in correlation with high IL-10 production and disease activity (*34*). Last, KO and KO-Tg nT_{reg} cells also expressed higher levels of OX-40 (fig. S4K), which has been shown to inhibit T_{reg} suppressive function (*35*).

To validate the functional significance of the differences in T_{reg} frequency and marker expression in KO and KO-Tg mice, we assessed their ability to suppress intestinal inflammation in a model of T cell–induced colitis. We have previously shown that T_{reg} cells from B6.*Sle1a* and B6.*Sle1a1* mice were less effective at suppressing intestinal inflammation induced by effector T (T_{eff}) cells in B6.*Rag-1*$^{-/-}$ mice (*11*, *12*). Yellow fluorescent protein–negative (YFP^-) non-T_{reg} cells from WT mice were transferred into B6.*Rag-1*$^{-/-}$ mice along with YFP^+ T_{reg} cells from WT, KO, or KO-Tg mice. KO and KO-Tg T_{reg} cell recipients showed a reduced body weight (Fig. 2C) and increased colon inflammation (Fig. 2D) as compared with the recipients of WT T_{reg} cells, suggesting that *Pbx1* deletion or *Pbx1-d* sole expression in T_{reg} cells led to reduced immune suppressive functions. In support of this hypothesis, we have previously shown that B6.*Sle1a* T_{reg} cells, which overexpress *Pbx1-d*, have a reduced ability to suppress of $CD4^+$ T_{eff} cell proliferation in vitro (*11*). The same result was obtained with Pbx1-KO YFP^+ T_{reg} cells, which showed a modest but statistically significant reduction in suppressive function (fig. S5).

Consistent with altered T_{reg} cell suppressive functions, T_{reg}-specific *Pbx1* deletion or *Pbx1-d* sole expression resulted in the spontaneous activation of non-T_{reg} $CD4^+$ T cells, with an increased expression of the early activation marker CD69 (Fig. 2, E and F) and other activation markers such as IL-2Rβ, GITR, OX-40, ICOS, and CD28 (fig. S4), as well as a small increase in pS6 expression, a marker of mTOR activation (fig. S4L). KO-Tg mice showed an accumulation of T_{FH} cells in both young and old mice, and it was also observed in old KO mice (Fig. 2, G and H). The frequency of follicular regulatory (T_{FR}) cells, nT_{reg}-derived population specific for germinal centers (GC), was also increased in parallel with that of T_{FH} cells (Fig. 2I). However, similar to T_{reg} cells (fig. S4A), *Pbx1* deficiency or *Pbx1-d* expression lowered FOXP3 expression in T_{FR} cells from old mice (Fig. 2J), which is likely to impair their function. Overall, these results suggest that *Pbx1* deletion or *Pbx1-d* sole expression reduced T_{reg} cell suppressive function, which resulted in an activation of $CD4^+$ effector T cells and an accumulation of T_{FH} cells.

In another T cell–driven autoimmune model, experimental autoimmune encephalomyelitis, B6.*Sle1a1* mice presented a more severe phenotype than B6 controls (*13*). Since clinical scores as well as the presence of interferon-γ (IFN-γ)– and IL-17A–producing T cells were partially rescued by retinoic acid, which induces iT_{reg} differentiation, it suggested that defective iT_{reg} cells expressing *Pbx1-d* contributed to this phenotype. Here, we showed that KO mice spontaneously accumulated with age IFN-γ–producing $CD4^+$ T cells while reducing the frequency of their IL-17A–producing $CD4^+$ T cells in the spleen (fig. S6, A and B).

Last, we assessed the effect of Pbx1 deficiency in ovalbumin (OVA)–induced hypersensitivity, a T helper cell 2 (T_H2)–driven inflammation

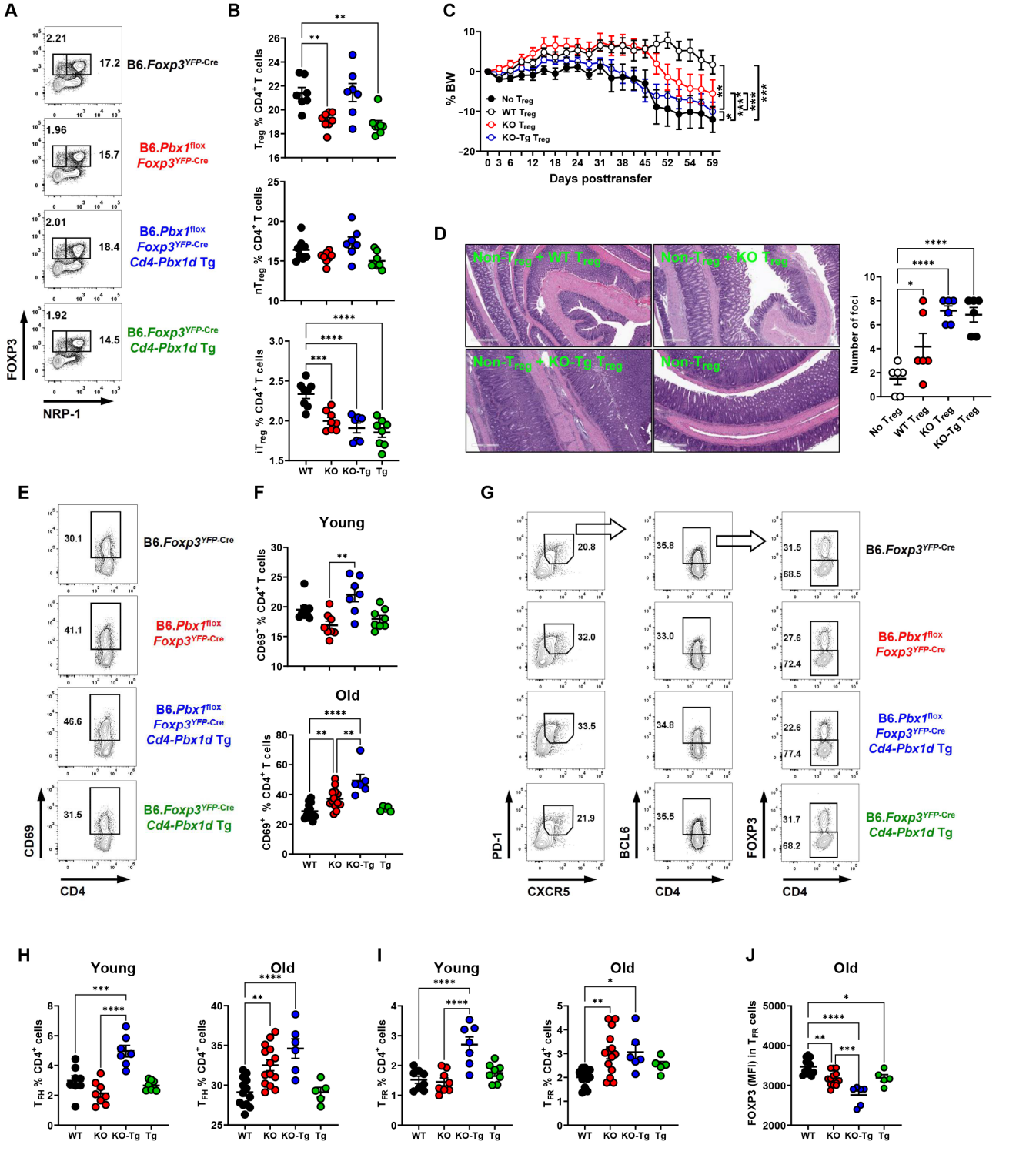

Fig. 2. *Pbx1* deletion or *Pbx1-d* sole expression decreased the peripheral T_{reg} cell population and their suppressive function. (**A** and **B**) Representative FACS plots (A) and frequency (B) of total splenic T_{reg} cells, $CD4^+FOXP3^+NRP\text{-}1^+$ nT_{reg} cells, and $CD4^+FOXP3^+NRP\text{-}1^-$ iT_{reg} cells. (**C** and **D**) WT non-T_{reg} cells were transferred into B6.*Rag-1*$^{-/-}$ mice without or with T_{reg} cells from WT, KO, or KO-Tg mice. (C) Changes in body weight (BW) after transfer. (D) Representative histopathology of hematoxylin and eosin–stained colons (original magnification: ×60, scale bar: 200 μm) for the four groups and corresponding number of foci. (**E** and **F**) Representative fluorescence-activated cell sorting(FACS) plots and frequency of splenic $CD69^+CD4^+$ T cells. (**G** to **J**) Representative FACS plots and frequency of splenic $CD4^+CXCXR5^+PD1^+BCL6^+FOXP3^-$ T_{FH} (H), $CD4^+CXCXR5^+PD1^+BCL6^+FOXP3^+$ T_{FR} cells (I) in $CD4^+$ T cells, and FOXP3 MFI in T_{FR} cells (J). Mean ± SEM of $N = 5$ to 14 3-month-old [graphs in (B) and young] mice and 8- to 10-month-old (old) mice compared with Dunnett's multiple comparisons tests. (C) and (D) Mean + SEM of $N = 6$ mice per group compared with two-way analysis of variance (ANOVA) (C) or Dunnett's multiple comparisons tests (D). $^*P < 0.05$, $^{**}P < 0.01$, $^{***}P < 0.001$, and $^{****}P < 0.0001$. PD-1, Programmed cell death protein 1.

of the lung in which T_{reg} cells play a protective role (*36*). The frequency of total $CD4^+$ T cells as well as $GATA3^+$ $CD4^+$ T (T_H2) cells was reduced in the lungs of KO mice (fig. S6, C to E). The frequency of total T_{reg} among $CD4^+$ T cells was not affected, but there was a trend for a reduced expression of $GATA3^+$ in these cells (fig. S6, F and G). As for the total T_{reg} cells, the frequency of nT_{reg} and iT_{reg} among $CD4^+$ T cells was similar between WT and KO mice (fig. S6, H and I). However, although there was still no difference for nT_{reg}, the frequency of iT_{reg} cells in $CD45^+$ cells was reduced in KO lungs and compared to WT, and there was a reduced iT_{reg}/nT_{reg} ratio (fig. S6, J to L). Consistent with a reduced frequency of $CD4^+$ T cells and T_H2 cells shown by flow cytometry, the lungs of KO mice showed a reduced inflammation and immune cell infiltrates (fig. S6M).

PBX1 regulates T_{reg} cell stability

The progressive decreased frequency of T_{reg} cells with *Pbx1* deficiency or *Pbx1-d* expression suggested that PBX1 may promote T_{reg} cell stability. The loss of FOXP3 expression leads to the production of FOXP3-negative ex-T_{reg} cells that have acquired inflammatory phenotypes, such as the production of IFN (*37*). To test whether *Pbx1*-d expression altered T_{reg} cell stability, we crossed T_{reg} cell–specific fate-mapping mice (B6.*Foxp3*$^{YFP\text{-}Cre}$.*R26R*^{RFP}) with *Pbx1-d* Tg mice. The frequency of $dTomato^+FOXP3^{neg}$ ex-T_{reg} cells was increased in the spleen and mLN from Tg.*R26R*^{RFP} mice compared with WT.*R26R*^{RFP} mice (Fig. 3, A and B), while there was no difference for the frequency of $dTomato^+FOXP3^+$ T_{reg} cells (Fig. 3C). The frequency ex-T_{reg} cells producing IFN-γ or IL-10 was similar between Tg and B6 mice (Fig. 3, D and E). However, since Tg mice produced more ex-T_{reg} cells, their frequency of IFN-γ^+ and IL-10^+ ex-T_{reg} among $CD4^+$ T cells was higher than in B6 (Fig. 3, F and G). There was no difference for IFN-γ production in T_{reg} cells (Fig. 3H), but Tg T_{reg} cells produced more IL-10, at least in the spleen (Fig. 3I). In addition, we observed an increased differentiation of T_{FH} cells from $FOXP3^+$ cells in $CD4^+CD44^+PD\text{-}1^+$-$CXCR5^+$ follicular cells (Fig. 3, J and K). The reporter system does not track whether these ex-T_{reg} T_{FH} cells differentiated directly from T_{FR} cells (losing FOXP3 and while maintaining BCL-6 expression) or from ex-T_{reg} cells (losing FOXP3 and acquiring BCL-6 expression). Together, our results indicated that the expression of the DN allele *Pbx1-d* promotes T_{reg} cell instability and the production of T_{FH} cells.

Pbx1 deletion and *Pbx1-d* sole expression in T_{reg} cells increased the humoral response to protein antigens

To determine whether *Pbx1* affects the humoral immune response to a T-dependent (TD) protein antigen, KO, KO-Tg, and Tg mice were immunized with 4-hydroxy-3-nitrophenylacetyl conjugated to keyhole limpet hemocyanin (NP-KLH) in alum, boosted 6 weeks after the first immunization and analyzed 1 week later. All the mice with *Pbx1*-altered T_{reg} cells showed increased frequency and number of $CD69^+CD4^+$ T cells and T_{FH} cells (Fig. 4, A and B). There was also an increased frequency of T_{FR} and T_{reg} cells in KO and KO-Tg immunized mice (Fig. 4, C and D), but as in old mice at steady state (Fig. 2J), the expression of FOXP3 was reduced in the T_{FR} and T_{reg} cells with altered *Pbx1* expression. There was a corresponding increased frequency and number, to a greater extent, of total GC B cells, NP-specific GC B cells, plasma cells, and NP-specific plasma cells (fig. S7). The production of high affinity NP-specific immunoglobulin G1 (IgG1), which is the main isotype produced against NP, mirrored the results obtained for T cells, with no difference for low affinity anti-NP IgG1 (Fig. 4E). KO-Tg mice also produced more high and low affinity NP-specific T_H1-driven NP-specific IgG2a and IgG2b. In addition, KO mice showed an enhanced production of low affinity anti NP-IgG2a and IgG2b (Fig. 4E). Overall, these results suggest that T_{reg} cells with a *Pbx1* deletion or *Pbx1-d* sole expression have reduced regulatory functions in TD humoral immune response.

Pbx1 deletion or *Pbx1-d* sole expression in T_{reg} cells increased T cell autoimmune responses

We tested the effect of *Pbx1* deficiency in T_{reg} cells in two models of lupus, one induced by the topical treatment with a Toll-like receptor 7 (TLR7) agonist (R848) (*38*) and a cGVHD induced by the transfer of MHC class II–disparate bm12 splenocytes (*39*). Shortly after TLR7 activation, KO and KO-Tg mice showed an increased frequency of $CD69^+CD4^+$ T cells, effector-memory $CD4^+$ T (T_{EM}) cells, T_{FH} cells, and plasma cells (Fig. 5, A to D). The cGVHD model also showed an increased frequency of activated $CD69^+CD4^+$ T cells and T_{EM} cells (Fig. 5, E and F), as well as an increased level of anti–double-stranded DNA (dsDNA) IgG production (Fig. 5G) with an increased specificity for dsDNA, as determined by *Crithidia* staining (Fig. 5H). These results suggest that *Pbx1* deletion or *Pbx1-d* sole expression in T_{reg} cells expanded autoreactive effector $CD4^+$ T cells during autoimmune responses.

Pbx1 deficiency altered gene expression in T_{reg} cells

To gain insights into how Pbx1 regulates T_{reg} cell maintenance and function, we performed RNA sequencing (RNA-seq) of $CD4^+FOXP3^+$ T_{reg} cells and $CD4^+CD44^+FOXP3^-$ T_{eff} cells sorted from KO and WT mice (fig. S8A). Principal components analysis (PCA) revealed that *Pbx1* deficiency in T_{reg} cells resulted in distinct transcriptional profiles in both T_{reg} and T_{eff} cells (fig. S8B). Some genes were differentially expressed in KO T_{reg} or T_{eff} cells only, and some genes in both (fig. S8C). Globally, 173 genes were up-regulated, and 111 genes were down-regulated in KO compared with WT T_{reg} cells (Fig. 6A). Gene set enrichment analysis (GSEA) showed that "positive regulation of transcription from RNA polymerase II promoter" was one of the top up-regulated pathways in KO T_{reg} cells, suggesting that Pbx1 may act mostly as a transcriptional repressor in T_{reg} cells (Fig. 6B). Genes and pathways related to apoptosis, cell proliferation, and cell cycle (Fig. 6, B and C) were also differentially enriched when *Pbx1* was deficient in T_{reg} cells. Compared to WT controls, KO T_{reg} cells had an increased expression of *Il10*, which confirmed the results obtained with protein expression (fig. S9C) and hyperactivation of Activator protein 1 (AP-1) transcription factors, including *Jun*, *Junb*, *Jund*, *Fos*, and *Fosb*, contributing to an enhanced transcription activity and cellular signaling. In addition, *Ascl2* (*40*) and *Runx2* (*41*), which promote T_{FH} cell differentiation, were also overexpressed in KO T_{reg} cells, potentially corresponding to the increased T_{FH} cells observed in Tg ex-T_{reg} cells. KO T_{reg} cells also showed an increased expression of *Bcl3*, which has been associated with defective T_{reg} cell function in colitis (*42*). *Fosl2*, a TCR-induced AP-1 transcription factor overexpressed in KO T_{reg} cells, represses T_{reg} development and promotes autoimmunity (*43*). CCAAT/enhancer binding protein promotes *Foxp3* stable expression in iT_{reg} cells (*44*). The increased expression of *Cebpa* and *Ceppb* in KO T_{reg} cells may correspond to a compensatory mechanism. In addition, a differentially expressed gene (DEG) cluster suggested an impaired migration of KO T_{reg} cells (fig. S8E), including the up-regulation of RGS genes, which have been shown to reduce chemoattractant sensitivity and cell migration in B cells (*45*).

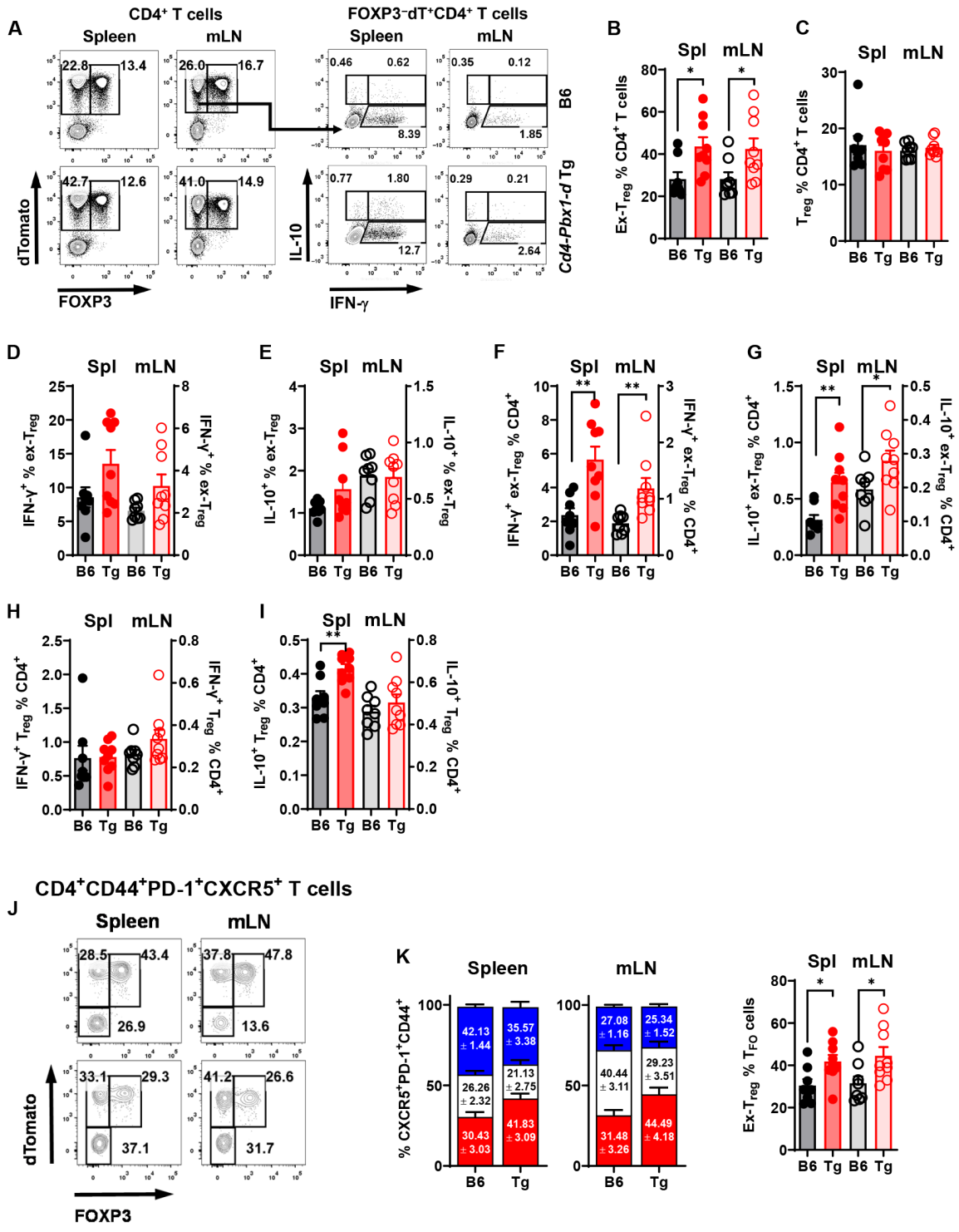

Fig. 3. *Pbx1-d* expression promotes T_{reg} instability. Representative FACS plots (**A**) and frequency of $CD4^+dTomato^+FOXP3^-$ ex-T_{reg} cells and $CD4^+dTomato^+FOXP3^+$ T_{reg} cells analyzed in $CD4^+$ T cells (**B** and **C**) in the spleen and mLN from 3-month-old B6.*R26R*^{RFP} and Tg.*R26R*^{RFP} mice. Frequency of IFN-γ^+ (**D**) and IL-10^+ (**E**) cells in ex-T_{reg} cells. Frequency of IFN-γ^+ ex-T_{reg} (**F**) and IL-10^+ ex-T_{reg} (**G**) in $CD4^+$ T cells. Frequency of IFN-γ^+ T_{reg} (**H**) and IL-10^+ T_{reg} (**I**) in $CD4^+$ T cells. Representative FACS plots (**J**) and frequency of ex-T_{reg} cells and T_{reg} cells in $CD4^+CD44^+PD\text{-}1^+CXCR5^+$ follicular T (T_{FO}) cells (**K**). The graphs on the left show distributions, and the graph on the right shows the comparison between ex-T_{reg} cells. Mean + SEM of $N = 8$ to 9 mice per group compared with *t* tests. $^*P < 0.05$ and $^{**}P < 0.01$.

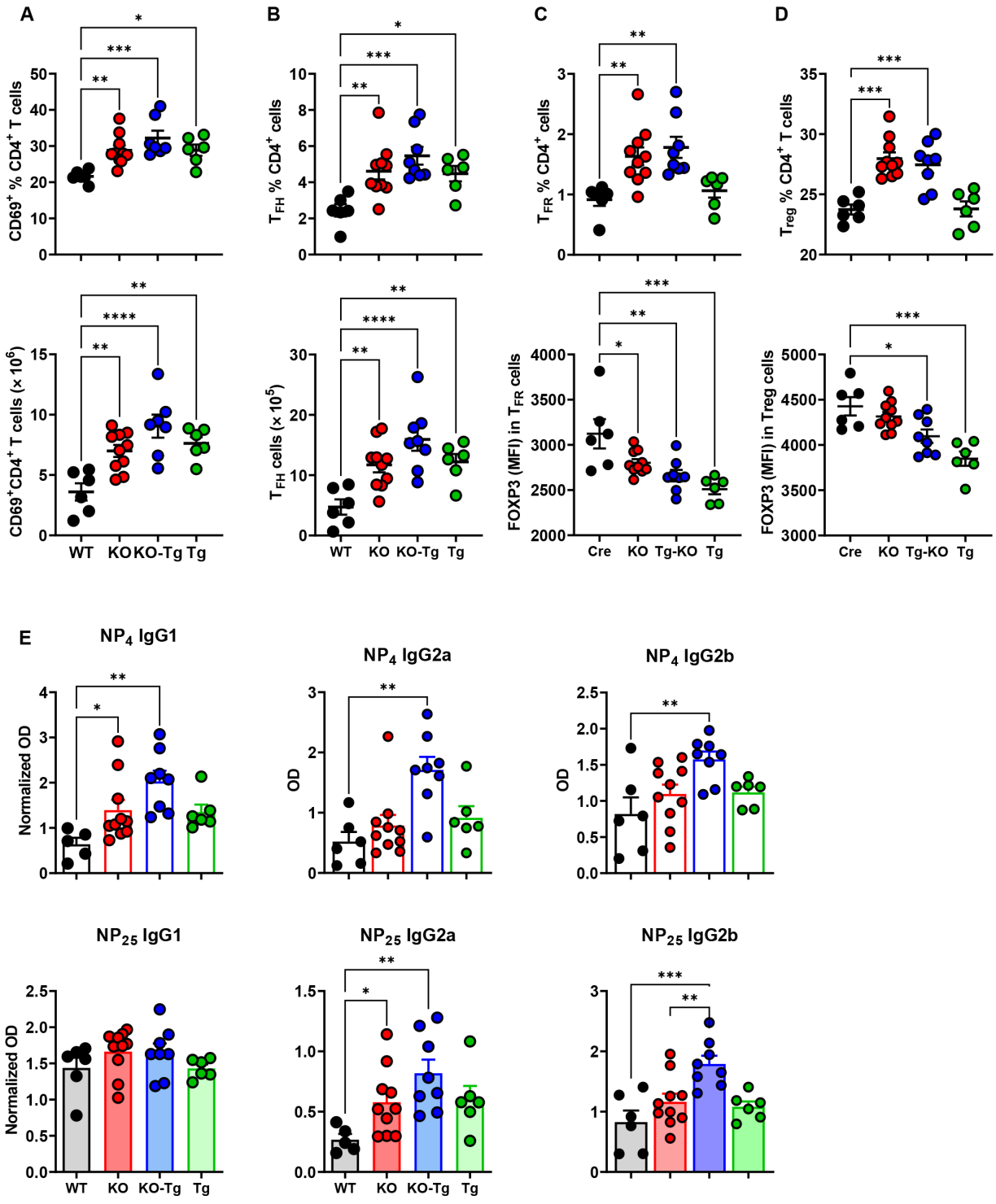

Fig. 4. T_{reg}cell–specific *Pbx1* deletion or *Pbx1-d* sole expression enhanced TD-humoral response. Mice were immunized with NP-KLH in alum, boosted 6 weeks later, and analyzed at week 7. (**A** and **B**) Frequency (top) and absolute number (bottom) of $CD4^+CD69^+$ cells (A) and T_{FH} cells (B). (**C** and **D**) Frequency (top) and FOXP3 mean fluorescence intensity (MFI) (bottom) in T_{FR} (C) and T_{reg} (D) cells. (**E**) Serum levels of high-affinity anti-NP_4 and low-affinity anti-NP_{25} IgG1, IgG2a, and IgG2b. Optical density (OD) values were normalized between three cohorts. Mean ± SEM of $N = 5$ to 10 mice per group performed in three cohorts, compared with Dunnett's multiple comparisons tests. *$P < 0.05$, **$P < 0.01$, ***$P < 0.001$, and ****$P < 0.0001$.

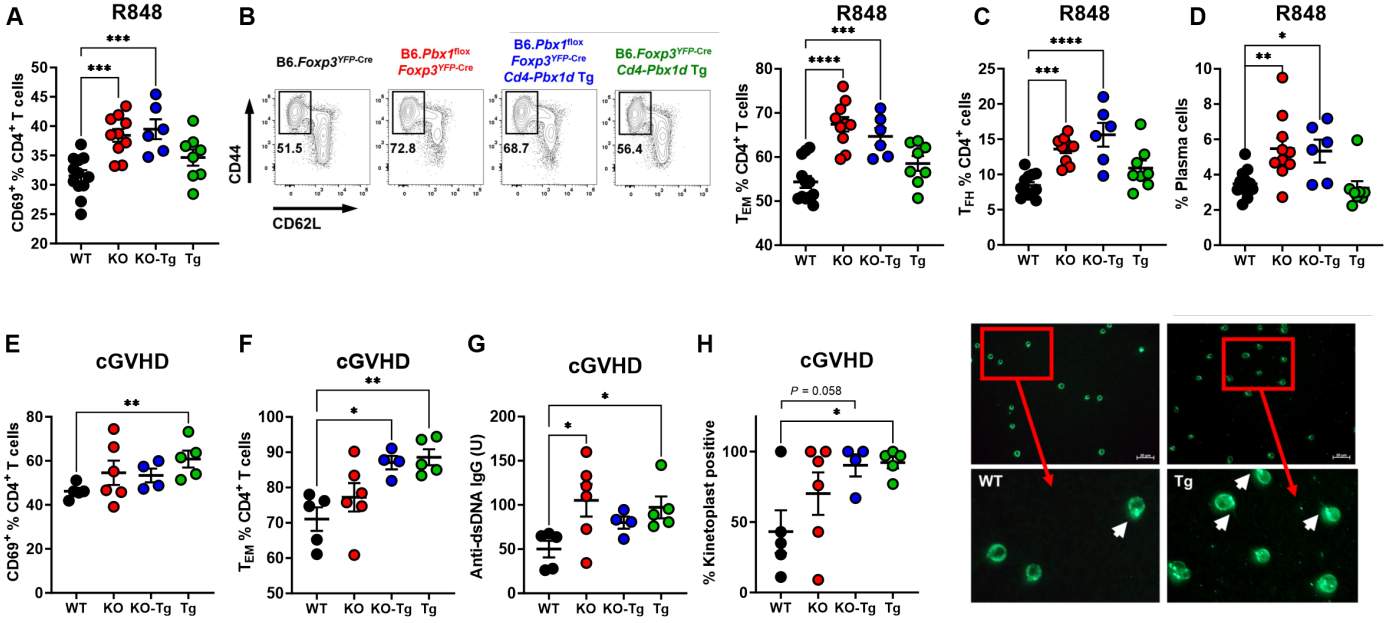

Fig. 5. *Pbx1* deletion or *Pbx1-d* sole expression in T_{reg} cells enhanced $CD4^+$ T cell autoimmune responses. (**A** to **D**) Mice were treated with R848 for 1 week and sacrificed at day 10. (A) Frequency of $CD4^+CD69^+$ cells. (B) Representative FACS plot and frequency of $CD4^+CD44^+CD62L^-$ T_{EM} cells. Frequency of T_{FH} cells (C) and IgD^-CD138^+ plasma cells (D). (**E** to **H**) cGVHD induced by transfer of B6.bm12 splenocytes into the four strains of recipient mice. Frequency of $CD4^+CD69^+$ cells (E) and T_{EM} cells (F). Levels of anti-dsDNA IgG (G) and anti-kinetoplast IgG positive *Crithidia* cells (H). The representative images in (H) show a *Crithidia* assay for a WT and a Tg recipient mouse with the low power showing the entire well, with magnification of the boxed areas. Arrows indicate anti-kinetoplast IgG-positive cells. Mean ± SEM of $N = 4$ to 12 mice per group compared with Dunnett's multiple comparisons tests. $^*P < 0.05$, $^{**}P < 0.01$, $^{***}P < 0.001$, and $^{****}P < 0.0001$.

Positive regulation of osteoblast differentiation, a pathway up-regulated in KO T_{reg} cells (Fig. 6B), has been associated with both *Pbx1* deficiency and *Pbx1-d* expression in a pre-osteoclast cell line (*21*), indicating shared pathways across cell types. The "cellular oxidant detoxification" was the top down-regulated pathway, which is informative since oxidative stress reported in T_{reg} cells in autoimmune settings, including SLE, promotes cell death and diminishes their suppressive function (*46*, *47*). A Hallmark pathway analysis of the KO T_{reg} cells also showed increased signaling and inflammatory responses with decreased fatty acid metabolism and oxidative phosphorylation, the main energy source in T_{reg} cells (fig. S8F), supporting that *Pbx1* deficiency impaired T_{reg} cell functions.

T_{eff} cells from KO mice showed 334 up-regulated and 114 down-regulated genes compared to T_{eff} cells from WT mice (Fig. 6D). Pathway analyses showed a marked enrichment for immune and inflammatory response genes, including *Ifng*, which was confirmed at the protein level (fig. S6, A and B) and *Il21*, as well as TCR signaling (Fig. 6E and fig. S9A). This confirmed the expansion of activated T cells observed at steady state (Fig. 2). The expression of chemokine receptors was highly disturbed with the down-regulation of *Ccr2*, *Crr4*, *Ccr5*, *Ccr6*, and *Ccr9* and the up-regulation of *Ccr8* (fig. S9B), suggesting, as for T_{reg} cells, changes in cell migration. In addition, *Ccr8* is critical for the expansion of proinflammatory $CD4^+CD52^{lo}$ T cells in patients with SLE and mice, which correlated with the frequency of circulating T_{FH} cells (*48*). These results show that *Pbx1*-deficient T_{reg} cells induce the expression of a proinflammatory transcriptional program in *Pbx1*-sufficient T_{eff} cells.

Il10 was one of the genes up-regulated in both T_{reg} and T_{eff} cells from KO mice (Fig. 6, A to D). *Cebpb* and *Fosl2*, also overexpressed in both T_{reg} and T_{eff} from KO mice, promote IL-10 expression across T cell subsets (*49*). IL-10 is of special interest since Pbx1 directly regulates its production in macrophages by binding to the *Il10* promoter (*50*). Moreover, excessive IL-10 production has been associated with SLE (*51*). The frequency of IL-10^+ T_{reg} cells was increased in KO mice (fig. S9, C and D), whereas there was no difference for non-T_{reg} cells (fig. S9E), suggesting *Pbx1*-independent posttranslational controls. Moreover, KO-Tg mice showed an increased frequency and number of both IL-10^+ T_{reg} and non-T_{reg} cells (fig. S9, C to E), suggesting that *Pbx1-d* sole expression in T_{reg} cells enhanced IL-10 production both directly and indirectly.

Pbx1 regulates cell proliferation by regulating *Rtkn2* expression

To better understand the mechanism by which Pbx1 regulates gene expression in T_{reg} cells, we focused on the 67 up-regulated and 71 down-regulated genes uniquely in KO T_{reg} cells (fig. S10, A and B). An in silico analysis identified putative Pbx1 binding sites in 113 of these genes (fig. S10B). Since cell proliferation and apoptosis were two major pathways regulated by Pbx1 in T_{reg} cells (Fig. 6, B and C), as it was reported in B cells (*19*), we focused on *Rhotekin2* (*Rtkn2*), which promotes cell cycle progression at the G_1 phase (*52*). *Rtkn2* has three predicted Pbx1 binding sites in the mouse promoter and two in the human promoter (fig. S11, A and B). *Rtkn2* expression was down-regulated in T_{reg} cells not in T_{eff} cells from KO mice (fig. S8D), which we confirmed at both the transcript and protein levels (Fig. 7, A and B). Next, we cotransfected human embryonic kidney (HEK) 293T cells with luciferase constructs containing the mouse *Rtkn2* promoter region with the two putative Pbx1 binding sites (fig. S11A) and expression plasmids for either the normal allele *PBX1-B* or the lupus DN allele *PBX1-D*. Both PBX1-B and PBX1-D

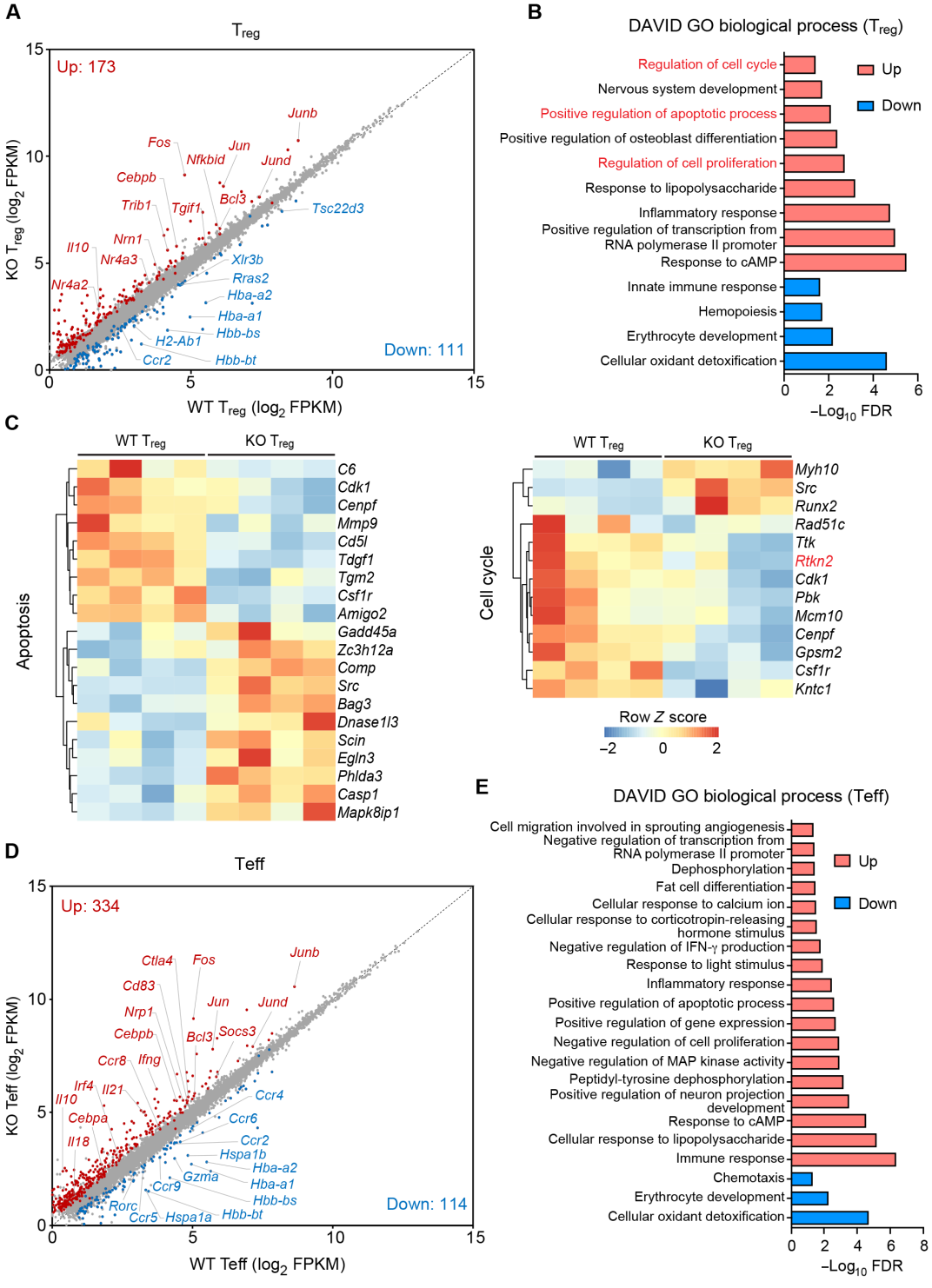

Fig. 6. Transcriptional regulation of T_{reg} and T_{eff} cells in mice with *Pbx1*-deficient T_{reg} cells. RNA-seq analysis was conducted on $CD4^+FOXP3^+$ T_{reg} cells and $CD4^+CD44^+FOXP3^-$ T_{eff} cells from WT and KO mice ($N = 4$). (**A**) Scatterplot of DEGs in T_{reg} cells. (**B**) GO biological processes enriched in genes that were up-regulated (top) or down-regulated (bottom) in KO T_{reg} cells. (**C**) Heatmap of DEGs in the apoptosis and cell cycle/proliferation pathways between WT and KO T_{reg} cells. (**D**) Scatterplot of DEGs in T_{eff} cells from WT and KO mice. (**E**) Database for Annotation, Visualization and Integrated Discovery Gene Ontology (DAVID GO) biological processes that were up-regulated or down-regulated in KO T_{eff} cells compared to WT controls. cAMP, cyclic adenosine 3′,5′-monophosphate; MAP, mitogen-activated protein.

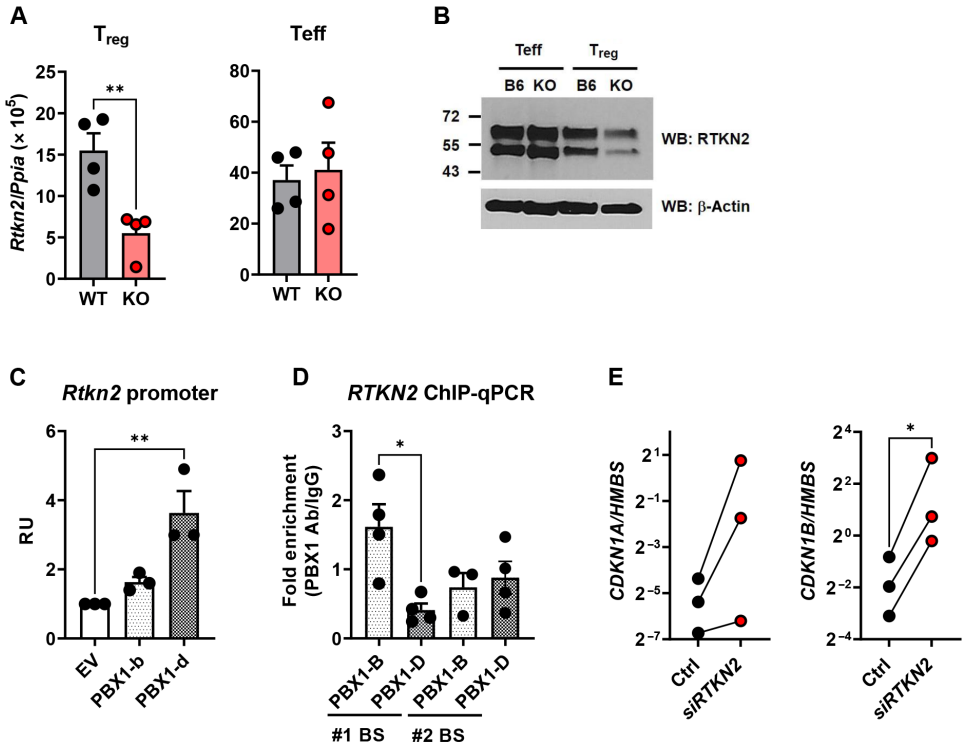

Fig. 7. *Pbx1* directly regulates *Rtkn2* expression. (A and **B**) *Rtkn2* gene (A) and RTKN2 protein (B) expression in T_{reg} and T_{eff} cells. $N = 4$. (**C**) Dual-luciferase analysis of murine *Rtkn2* expression in HEK293T cells in the presence of PBX1-B or PBX1-D, showing fold change relative to the control expression plasmid [empty vector (EV)]. (**D**) ChIP-qPCR analysis of the human *RTKN2* promoter in *PBX1-B* or *PBX1-D* overexpressing Jurkat T cells. Results are shown relative to the IgG control. $N = 3$ to 4. (**E**) *CDKN1A* and *CDKN1B* expression normalized to *HMBS* in Jurkat T cells treated with siRTKN2 or si control. $N = 3$. Mean + SEM compared with *t* tests $^*P < 0.05$ and $^{**}P < 0.01$. Ab, antibody. WB, Western blot; RU, relative unit; BS, binding site.

increased *Rtkn2* transcription with higher levels obtained for PBX1-D (Fig. 7C). This indicated that PBX1 directly regulates *Rtkn2* transcription. PBX1 either transactivates or represses gene expression depending of the presence/absence of cofactors (*14*). Our results suggests that while *Rtkn2* expression is reduced by *Pbx1* deficiency in T_{reg} cells, *Rtkn2* expression was promoted by the DN allele in HEK293T epithelial cells. Chromatin immunoprecipitation–quantitative polymerase chain reaction (ChIP-qPCR) analysis of Jurkat T cells overexpressing PBX1-B or PBX1-D showed that PBX1-B but not PBX1-D binds to the upstream putative PBX1 binding site 1 in the promoter of human *RTKN2* (Fig. 7D and fig. S11B). Putative binding site 2 did not show evidence of PBX1 binding, although its sequence similarity to the consensus PBX1 binding sequence was equivalent to that of binding site 1 (fig. S11C). This suggests that cofactors may be recruited at site 1 but not 2. Last, we confirmed that RTKN2 promotes cell proliferation by showing that *RTKN2* knockdown in Jurkat T cells increased the expression of *CDKN1A* and especially *CDKN1B*, two cyclin kinase inhibitors that enforce G_1 phase cell cycle arrest (Fig. 7E). Overall, these results strongly support a direct transcriptional regulation of *Rtkn2* by Pbx1 in T_{reg} cells. Since Rtkn2 promotes proliferation, its decreased expression in *Pbx1* KO and lupus T_{reg} cells suggests that it may be one of the target genes through which Pbx1 regulates cell cycle in this cell type.

Pbx1 regulates T_{reg} cell proliferation

To test the hypothesis that *Pbx1* regulates T_{reg} cell proliferation, we compared T_{reg} cell proliferation ex vivo between the four strains of *Pbx1* mice. The frequency of Ki-67$^+$ proliferating T_{reg} cells was decreased in KO, KO-Tg, and Tg mice as compared to WT, whereas non-T_{reg} cells showed no difference between strains (Fig. 8, A to C). T_{reg} cells from KO mice also showed a greater expression of both *Cdkn1a* and *Cdkn1b*, while there was no difference in Teff cells (Fig. 8D). Last, Jurkat T cells overexpressing *PBX1-D* also showed an increased frequency of cells in G_1 phase with a corresponding decreased in S phase (Fig. 8, E and F), suggesting that PBX1-D suppressed cell proliferation via G_1 phase cell cycle arrest. Overall, our results indicate that PBX1 supports T_{reg} cell proliferation through RTKN2 by inhibiting the expression of *CDKN1A* and *CDKN1B*, allowing cell cycle progression.

DISCUSSION

SLE pathogenesis has been associated with defects in T_{reg} cells as well as an expansion of T_{H1} and T_{FH} cells in multiple murine and human studies (*53*). There is strong evidence that T_{reg} cells control the T_{FH} cell pool, either directly or indirectly through the T_{FR} population (*54*), which may be one of the mechanisms by which alterations in T_{reg} cells contribute to SLE pathogenesis. Regardless of the mechanisms, the success of T_{reg} cell adoptive therapy in one SLE patient (*55*), as well as recent clinical trials in which patients with SLE received low-dose IL-2 to expand T_{reg} cells (*56*), indicates their significance as therapeutic targets.

Inflammatory cytokines that are common contributors to lupus pathogenesis, such as IL-6 or type I IFN, impair T_{reg} functions

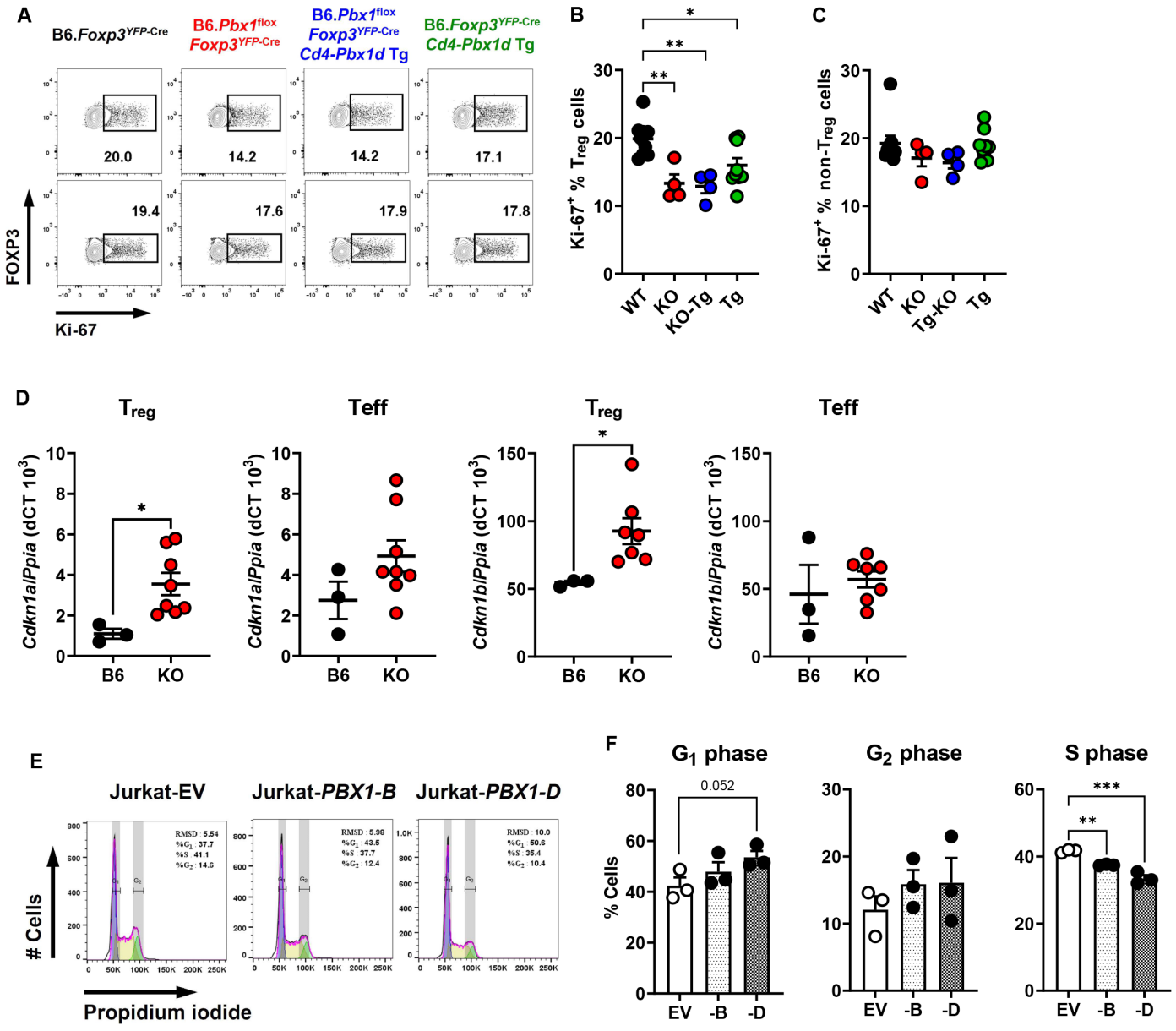

Fig. 8. *Pbx1* regulates cell proliferation in T_{reg} cells. Representative FACS plot (**A**) and frequency of Ki-67$^+$ cells in T_{reg} (**B**) and non-T_{reg} (**C**) cells from WT, KO, KO-Tg, or Tg mice. Mean ± SEM of $N = 4$ to 9 3-month-old mice per group compared with Dunnett's multiple comparison tests. (**D**) *Cdkn1a* and *Cdkn1b* expression in T_{reg} and Teff cells from WT and KO mice. Mean ± SEM of $N = 3$ to 8 3-month-old mice per strain compared with Mann-Whitney tests. Representative FACS histograms of propidium iodide staining relative to cell cycle phases (**E**) and corresponding frequency (**F**) in *PBX1-B* or *PBX1-D* overexpressing Jurkat T cells as compared to empty vector controls. Mean + SEM of $N = 3$ compared with *t* tests. *$P < 0.05$, **$P < 0.01$, and ***$P < 0.001$. RMSD, root mean square deviation.

(*57*, *58*). There is also evidence for a genetic basis for impaired T_{reg} cells in lupus (*8*), including the *Esrrg* and *Pbx1* genes in the *Sle1* murine susceptibility locus, which has the strongest linkage to lupus nephritis and directs the production of autoantibodies through intrinsic defects in B and CD4$^+$ T cells (*59*, *60*). The low expression of *Esrrg* in T cells corresponds to the *Sle1c2* locus (*61*), and *Esrrg* deletion in T_{reg} cells impaired their suppressive function and led to the expansion of autoreactive inflammatory Teff cells (*62*). The overexpression of the DN allele *Pbx1-d* in T cells, which corresponds to *Sle1a*, impaired T_{reg} cell differentiation and maintenance and favored T_{FH} cell differentiation (*11*, *13*, *24*).

The present study specifically examined the role of Pbx1 in T_{reg} cells. We showed that T_{reg} cells express a higher level of *Pbx1* as compared to non-T_{reg} CD4$^+$ T cells, for reasons that are not yet known. We have shown that *Pbx1* expression was reduced in both CD4$^+$ T cells and B cells upon receptor stimulation (*63*), which may contribute to a relatively higher expression in T_{reg} cells. Further, T_{reg} cells from both lupus-prone mice and patients with SLE expressed lower amounts of *Pbx1* as compared to their healthy counterparts. FOXP3-specific *Pbx1* deletion or *Pbx1-d* sole expression in T_{reg} cells reduced T_{reg} cell differentiation and immune suppressive functions, leading to a selective accumulation of effector CD4$^+$ T cells favoring T_{H1} at steady state and T_{FH} cells upon

challenge, with a relative suppression of T_H2 and T_H17 cells. The mechanism responsible for this selective targeting is unclear. In addition, transcriptome analysis identified alterations in cell migration pathways for both KO T_{reg} cells and the corresponding Teff cells, which matched the altered recruitment of $CD4^+$ T cells to the lung upon inflammation as well as to the gut under homeostatic conditions that were observed in this study. Tissue specificity, which is known to shape T_{reg} cell phenotype and function, may further affect the effect of *Pbx1* on T_{reg} cells. These multiple layers of complexity warrant additional studies to be untangled.

We showed that *Pbx1* expression was not required for T_{reg} cells to differentiate either in vivo or in vitro. Furthermore, analysis of T_{reg} subsets as well as fate-mapping constructs suggested that *Pbx1* deficiency or *Pbx1-d* expression impaired the maintenance of peripheral T_{reg} cells. *Pbx1* deficiency and *Pbx1-d* expression, either endogenous in mice carrying the NZW-derived *Sle1a1* locus or as a Tg, have overlapping but not identical effects on T_{reg} cells, and the strongest phenotypes were obtained for T_{reg} cells in which *Pbx1-d* Tg was expressed in the absence of other isoforms. In addition to functioning as a DN isoform, Pbx1-d may bind to regulatory regions indirectly through cofactors, which could explain the differences between the KO and Tg T_{reg} cells. While the analysis of *Pbx1* deficiency unveiled the role of Pbx1 in T_{reg} cells, *Pbx1-d* needs to be characterized relative to *Pbx1-b* as the isoform associated with lupus susceptibility. Only unbiased genomic studies comparing the chromatin landscape and gene expression under *Pbx1* deficiency or the sole expression of either isoform in T_{reg} cells will define their role in T_{reg} homeostasis.

Transcriptome analysis identified cell proliferation and apoptosis as major pathways altered by *Pbx1* deficiency in T_{reg} cells. *Rtnk2* was one of the genes whose expression was greatly reduced by *Pbx1* deficiency in T_{reg} but not in Teff cells. RTKN2 is a Rho-GTPase effector protein that regulates cell survival and cell cycle progression (*64*) and that is highly expressed in human peripheral T cells as compared to other immune cells (*65*). Among human $CD4^+$ T cells, T_{reg} cells express the highest *RTKN2* expression, and knocking down *RTKN2* expression impaired T_{reg} functions while *RTKN2* overexpression protected conventional T cells from T_{reg} suppression of proliferation (*66*). RTKN2 was previously reported to prevent apoptosis in $CD4^+$ T cells through nuclear factor κB (NF-κB) activation and BCL-2 expression (*67*). Furthermore, *RTKN2* gain-of-function variants have been associated with rheumatoid arthritis through NF-κB activation (*68*). The activation of the NF-κB pathway is required for the differentiation and function of T_{reg} cells (*69*). More specifically, p65 RelA regulates the expression of T_{reg} gene signature (*70*), and p65-deficient T_{reg} cells are unstable with defective suppressive function (*71*). A reduced *Rtkn2* expression in Pbx1 KO T_{reg} cells is predicted to reduce p65 expression, resulting in a partial overlap between Pbx1 and p65 KO T_{reg} cells. RTKN2 also promoted proliferation (*72*) and resistance to apoptosis (*73*) in tumor cells through the Wnt/β-catenin pathway. However, since Wnt/β-catenin signaling impairs T_{reg} cells by interfering with FOXP3 transcriptional activity (*74*), it is unlikely that *Pbx1* regulates T_{reg} cell proliferation through *Rtkn2* via Wnt/β-catenin signaling.

We showed that *Pbx1* directly regulates *Rtkn2* expression. As previously shown in human T_{reg} cells, we showed here that *Pbx1*-deficient T_{reg} cells have an impaired suppressive function, reduced proliferation, and stability. These results suggest that Pbx1 has a critical role in the homeostatic maintenance of T_{reg} cells, at least partially by maintaining *Rtkn2* expression. Pbx1 may regulate T_{reg} cells through mechanisms other than proliferation and resistance to apoptosis. Pbx1 directly up-regulates *Nfil3* expression in CLPs for NK cells to differentiate (*75*), and NFIL3 regulates the expression of *Foxp3* and other T_{reg}-associated genes (*76*). Pbx1 may therefore also regulate T_{reg} cells through NFIL3. Other direct Pbx1 putative targets differentially expressed the T_{reg} cells of Pbx1 KO mice have also the potential to play a critical role. It is noteworthy that, contrary to T_{reg} cells and most tumor cells, *Pbx1* deficiency in B cells increased their proliferation, which is associated with lupus phenotypes (*19*). It is known that the interplay with a complex array of cofactors results in Pbx1 functioning either as a transcriptional activator or repressor. Overall, these two studies show that the low expression of *Pbx1* found in the lymphocytes of patients with SLE as well as the expression of its DN allele Pbx1-d in T cells contribute to pathogenesis through at least two cell types, B cells and T_{reg} cells, in which the cell cycle regulation is impaired, although in opposite directions.

MATERIALS AND METHODS

Experimental design

We evaluated the expression of the *Pbx1* gene and its *Pbx1-d* isoform in T_{reg} and non-T_{reg} T cells sorted from the peripheral blood of patients with SLE and HCs and from the spleen of lupus-prone mice and HCs using quantitative reverse transcriptase PCR (qRT-PCR). We produced a mouse strain in which *Pbx1* was deleted in T_{reg} cells (KO), a strain in which *Pbx1-d* was overexpressed in total T cells (Tg), as well as a strain in which *Pbx1-d* was the only *Pbx1* isoform expressed in T_{reg} cells (KO-Tg). We used flow cytometry to compare the frequency and phenotypes of T_{reg} and Teff cells in the spleen and thymus of these mice to that of WT controls. The suppressive function of these T_{reg} cells was evaluated in an induced colitis model. The stability of the Tg T_{reg} cells was analyzed in mice carrying a fate-mapping construct to track T_{reg} cells that have lost FOXP3 expression. The enhanced effector functions of Teff cells that developed in these strains were evaluated by flow cytometry and antibody measurements in response to protein immunization as well as in two induced models of lupus. Gene expression in sorted T_{reg} and Teff cells from the KO and WT mice was evaluated by RNA-seq. The specific down-regulation of *Rtkn2* in KO T_{reg} cells was validated by qRT-PCR and Western blotting. Binding of the PBX1-B normal isoform and PBX1-D DN isoform on the *RTKN2* promoter was compared with a luciferase assay and a ChIP assay in Jurkat T cells overexpressing each of these isoforms. *RTNK2* expression was knocked down in Jurkat T cells with small interfering RNA (siRNA), and the expression of cyclin kinase inhibitors *CDKN1A* and *CDKN1B* was measured by qRT-PCR. T_{reg} cell proliferation was evaluated ex vivo by flow cytometry for KI-67 staining in the T_{reg} and non-T_{reg} T cells of KO, Tg, KO-Tg, and WT mice. Cell cycle analysis was performed in Jurkat T cells overexpressing either the PBX1-B or PBX1-D isoforms by flow cytometry.

Mice

C57Bl/6J (B6), B6.129S-*Pbx1*$^{tm3.1Mlc}$/J (B6.Pbx1$^{f/f}$), B6.Cg-Tg(Cd4-cre)1Cwi/BfluJ (CD4-Cre), (NZB x NZW)F1 (BWF1), BXSB.*Yaa*, B6(C)-*H2-Ab1*^{bm12}/KhEgJ (B6.bm12), B6.129(Cg)-*Foxp3*$^{tm4(YFP/icre)Ayr}$/J (B6.*Foxp3*$^{YFP\text{-}Cre}$), B6.Cg-*Gt(ROSA)26Sor*$^{tm9(CAG\text{-}tdTomato)Hze}$/J (R26R^{RFP}), B6.SJL-*Ptprc*^{a} *Pepc*^{b}/BoyJ (B6.CD45.1), and B6.*Rag-1*$^{-/-}$ mice were originally obtained from The Jackson Laboratory. B6.NZM-*Sle1*$^{NZM2410/Aeg}$*Sle2*$^{NZM2410/Aeg}$*Sle3*$^{NZM2410/Aeg}$/LmoJ (TC) congenic mice (*77*) and B6.*Cd4-Pbx1-d* Tg mice with *Pbx1-d* overexpression

controlled by the *Cd4* promoter (*24*) have been previously described. B6.*Foxp3*$^{YFP\text{-}Cre}$.*Pbx1*$^{f/f}$ (KO mice) carry a T_{reg}-specific *Pbx1* deletion. KO-Tg were generated to have T_{reg} cells expressing solely the *Pbx1-d* isoform. To control for Foxp3$^{YFP\text{-}Cre}$ expression, B6.*Foxp3*$^{YFP\text{-}Cre}$ mice were used as WT and B6.*Foxp3*$^{YFP\text{-}Cre}$.*Cd4-Pbx1-d* Tg as Tg. B6.*Cd4*^{Cre}.*Pbx1*$^{f/f}$ (Pbx1$^{CD4\text{-}KO}$) mice carry a *Pbx1* deletion in all T cells, with CD4-Cre mice used as controls. Experiments were performed with female mice except for BXSB.*Yaa* males. "Young" mice were 3 months old, and "old" mice were 8 to 10 months old. All mice were bred and maintained at the University of Florida (UF) and the University of Texas Health San Antonio (UTHSA) in specific pathogen–free conditions with Institutional Animal Care and Use Committee approval from both institutions.

Human subjects

Female patients with SLE fulfilling at least four 1997 American College of Rheumatology criteria for SLE were enrolled at the UF Lupus clinic. Peripheral blood was obtained from 10 patients with SLE and 7 female HCs after informed consent was obtained in accordance with an UF Institutional Review Board approved protocol (UF IRB approval 201300225). The patients presented with stable disease and low SLE Disease Activity Index of 3 to 4, and they were treated with conventional treatments.

Flow cytometry

Single-cell suspensions were prepared from spleen, mLN, thymus, as well as lamina propria from the small intestine and the colon using standard procedures. After red blood cell lysis, cells were blocked with anti-CD16/32 antibody (2.4G2) and stained in fluorescence-activated cell sorting (FACS) staining buffer [2.5% fetal bovine serum (FBS) (Genesee Scientific) and 0.05% sodium azide in phosphate-buffered saline (PBS) (Corning)]. Fluorochrome-conjugated antibodies used in this study were listed in table S1. Follicular T cells were stained as previously described (*24*) in a three-step process using purified CXCR5 (2G8) followed by biotinylated anti-rat IgG (Jackson ImmunoResearch Laboratory) and then Peridinin-Chlorophyll-Protein (PerCP)-labeled streptavidin in a FACS staining buffer on ice. For cell cycle analysis, cells fixed with 70% ethanol were stained for DNA content with the FxCycle propidium iodide/RNAase staining solution (Thermo Fisher Scientific) following the manufacturer's instructions. For intracellular staining, cells were fixed and permeabilized with FOXP3 staining buffer (Thermo Fisher Scientific) according to the manufacturer's protocol. NP-phycoerythrin was purchased from Biosearch Technology. Dead cells were excluded with fixable viability dye (eFluor780; Thermo Fisher Scientific). Data were collected on LSRFortessa (BD Biosciences) at the Flow Cytometry Shared Resource at UTHSA and analyzed with FlowJo software (Tree Star).

In vivo treatments

Colitis was induced as previously described (*12*). Briefly, 4×10^5 $CD4^+CD25^-$ Teff cells from WT mice were transferred with KO, KO-Tg, or WT 1×10^5 T_{reg} cells into 2-month-old B6.*Rag-1*$^{-/-}$ mice. Body weight was recorded at least weekly for 60 days, when the mice were euthanized and colon was processed for hematoxylin and eosin stain. The number of foci per section was counted in a blind fashion. For TD immunization, 8- to 10-week-old mice were intraperitoneally injected 100 μg of NP(31)-KLH (Biosearch Technology) in alum (1:1), boosted with the same Ag in alum 6 weeks later, and analyzed 1 week after the boosting immunization. In the TLR7 activation model, mice were treated with 100 μg of resiquimod (R488, Tocris) in 100 μl of acetone (Thermo Fisher Scientific) by topical application to the right ear on days 0, 2, and 6, and sacrificed at day 10 to analyze the phenotype of splenocytes. cGVHD was induced according to an established protocol (*39*). Briefly, 5 to 8×10^7 splenocytes from B6.bm12 mice were intraperitoneally transferred into WT, KO, KO-Tg, and Tg mice. Mice were sacrificed 6 weeks later to assess serum autoantibodies and splenic $CD4^+$ T cell phenotypes.

To induce OVA hypersensitivity, 2-month-old WT and KO mice were sensitized with 50 μg of OVA (Sigma-Aldrich) in 0.1 ml of 2% Alhydrogel (InvivoGen) and 0.4 ml of sterile PBS via intraperitoneal injection. Sensitized mice were exposed for 45 min daily to aerosolized solutions of either 1% OVA or PBS from day 15 to 19 and then were sacrificed on day 21. After a bronchoalveolar lavage with 1 ml of PBS, the left main bronchus was clamped, and the left lung was excised to be processed for flow cytometry. One lobe was digested with the Lung Dissociation Kit (Miltenyi Biotec). Five hundred microliters of enzyme solution was injected into the lobe before mechanical dissociation in 2.5 ml of enzyme solution using the gentleMACS Octo Dissociator with Heaters (Miltenyi Biotec). After dissociation, immune cells were collected between a 33 and 66% Percol (Cytiva) gradient in RPMI 1640 (Corning) containing 2% FBS. The right lung was infused with 1 ml of 10% neutral-buffered formalin and fixed for 24 hours before paraffin embedding and hematoxylin and eosin staining. Imaging was performed with a B-ZX 100 Keyence microscope. The surface area of the infiltrate calculated with the same threshold for all samples was expressed as percentage of the total tissue area.

In vitro T cell assays

For T_{reg} polarization, total $CD4^+$ T cells isolated from Pbx1$^{CD4\text{-}KO}$ and $CD4^{Cre}$ mice by negative selection with the $CD4^+$ T Cell Isolation Kit (Miltenyi Biotec) were cultured (1×10^6 per well) for 4 days in 24-well plates coated with plate-bound anti-CD3e (4 μg/ml; 145-2C11, BD Biosciences) and complete RPMI 1640 media supplemented with anti-CD28 antibody (1 μg/ml; 37.51, BD Biosciences), TGF-β (3 ng/ml; PeproTech), IL-2 (50 ng/ml R&D Systems), anti–IFN-γ (10 ng/ml; XMG1.2, BioXcell), and anti-IL-4 (10 μg/ml; 11B11, BioXcell).

$FOXP3^-YFP^+$ T_{reg} and $FOXP3^-YFP^-$ Teff cells were sorted from negatively selected $CD4^+$ T cells) using a FACSAria sorter, and $FOXP3^-YFP^-$ Teff cells isolated from WT mice were labeled with CellTrace Violet (CTV) (Life Technologies, Thermo Fisher Scientific). Dendritic cells (DCs) were isolated from B6.CD45.1 mice by positive selection with an anti-CD11c isolation kit (Miltenyi Biotec). T_{reg} cells were incubated with Teff cells (1×10^5) at a 1:1 to 1:8 ratio in the presence of 1×10^4 DCs and soluble anti-CD3e antibody (1 μg/ml; BD Biosciences, 145-2C11) for 3 days. The proliferation of Teff cells was determined by CTV dilution.

Antibody measurements

Serum NP-specific antibodies were measured by enzyme-linked immunosorbent assay using plates coated with NP(4)– or NP(25)–bovine serum albumin (high or low affinity, respectively) (Biosearch Technology), followed by incubation with 1:1000 diluted serum samples, and developed with alkaline phosphatase-conjugated goat anti-mouse IgG, IgG2a, or IgG2b (Southern Biotech) as previously described (*78*). Anti-dsDNA IgG were measured as previously described (*79*) in sera diluted 1:500, and relative units were standardized using serial dilutions of pooled sera from TC mice, setting the 1:100 dilution reactivity to

100 U. All samples were run in duplicate. To analyze the specificity of anti-dsDNA IgG for dsDNA, serum was diluted 1:10 for *Crithidia luciliae* indirect immunofluorescence test (Bio-Rad) followed by incubation with goat anti-mouse IgG–fluorescein isothiocyanate antibody (Southern Biotech) in triplicates. The images were acquired on an inverted fluorescence microscope (Olympus). The results were quantified as the percentage of *Crithidia* cells showing a well-defined kinetoplast in a blind manner and then averaged between triplicates.

RNA-seq and RT-PCR

RNA for RNA-seq was extracted from sorted T_{reg} cells ($CD4^+FOXP3^+$) and Teff cells ($CD4^+CD44^+FOXP3^-$) of 2- to 3-month-old WT and KO mice using the RNeasy Plus Micro Kit (Qiagen) and subsequent used for full-length cDNA synthesis using a SMART-Seq HT kit (Takara). RNA-seq libraries were prepared, and data were analyzed essentially as described previously (*80*). Briefly, raw sequence reads were aligned to the mouse reference genome (GRCm38) using STAR v2.7.5c. Normalized counts (FPKM, fragments per kilobase of transcript per million mapped reads) values were used for PCA and heatmap plotting in R. DESeq2 was used to determine significantly expressed genes (DEGs) based on the following criteria: FPKM > 1, false discovery rate < 0.05, fold change > 1.5. GSEA was conducted using DAVID (https://david.ncifcrf.gov/), and redundant gene ontology terms were removed using REVIGO (http://revigo.irb.hr/). For qRT-PCR analyses, murine T_{reg} and non-T_{reg} $CD4^+$ T cells were sorted from splenocytes of WT and KO mice based on Foxp3-YFP expression and from non-Tg mice as $CD4^+CD25^{hi}$ cells. Human T_{reg} and non-T_{reg} $CD4^+$ T cells were isolated form PBMCs of patients with SLE and HCs using the $CD4^+CD25^+CD127^{dim/-}$ Regulatory T Cell Isolation Kit II (Miltenyi Biotec). RNA was extracted with an RNeasy Micro kit (Qiagen), and cDNA was synthesized from 200 to 500 ng total RNA using the ImProm-II Reverse Transcription system (Promega). PCR amplification was performed using SYBR Green Supermix (Bio-Rad) with primers listed in table S2. Normalization to housekeeping gene *HMBS* (human) or *Ppia* (mouse) was carried out with the $2^{\Delta\Delta Ct}$ method. Primer sequences are listed in table S2.

Chromatin immunoprecipitation–quantitative polymerase chain reaction

ChIP was performed on *PBX1-B* or *PBX1-D* overexpressing Jurkat T cells (*21*) with a ChIP assay kit (Millipore-Sigma), according to the manufacturer's instructions with an anti-PBX1 polyclonal antibody or normal rabbit IgG (both Cell Signaling) as control. Putative PBX1 binding sites in the human *RTKN2* promoter were identified using Jaspar3 (set for 75% accuracy), and primers designed for Chip-qPCR around these sites (fig. S8) are listed in table S2.

Luciferase assay

Two putative Pbx1 binding sites in the ~1 kb upstream from exon 1 in the murine *Rtkn2* promoter region were identified using Jaspar3 (fig. S8). We generated a 791-bp luciferase reporter construct cloned into the pGL4.25 Luciferase vector (Promega). *PBX1-B* or *PBX1-D* expression pcDNA3 plasmids were purchased from Origene. HEK293T cells were cotransfected with *Rtkn2* pGL4.25 with *PBX1-B* or *PBX1-D* expression plasmids using the Lipojet transfection kit (Ver.II) (SignaGen Laboratories). After 48 hours, cells were harvested and lysed with passive lysis buffer (Promega), and firefly and renilla luciferase activities were measured using a dual-luciferase reporter assay system (Promega), according to the manufacturer's instructions. The results were presented as firefly/renilla luciferase activities.

RTKN2 siRNA knockdown and cell cycle analysis

Dharmacon Accell predesigned siRNA for human *RTKN2* SMART pool with Accell *GAPDH* control pool was purchased from Horizon. Jurkat T cells were harvested and washed twice with Accell delivery media. One million cells were mixed with each siRNA SMART pools at a final concentration of 1 μM in 24 well-plates and incubated for 3 days. RNA was isolated to measure *RTKN2* expression. For stable expression of the PBX1-B and PBX1-D isoforms in Jurkat T cells (ATCC), 2×10^5 cells were electroporated with the SE Cell Line 4D-Nucleofector X Kit S using selected program CL-120 (Lonza). A total of 0.4 μg of pcDNA-PBX1-B or pcDNA-PBX1-D expression plasmids (Origene) with selectable marker for geneticin (G418) was added to cells. An empty plasmid was used as control. After electroporation, cells were cultured in complete RPMI with G418 (500 μg/ml) for 3 days. PBX1 expression was confirmed by Western blotting using a PBX1 primary antibody (Cell Signaling). These Jurkat-PBX1-B, Jurkat-PBX1-D, and control cells were used for cell cycle analysis.

Western blot

FACS-sorted murine T_{reg} and Teff cells were lysed in lysis buffer [50 mM tris-Cl (pH 7.4), 150 mM NaCl, 2 mM EDTA, and 0.5% Triton X-100 including protease inhibitor cocktail]. Lysates were briefly sonicated, incubated for 30 min on ice, and precipitated at 12,000 rpm for 20 min. Twenty to 30 μg of the soluble fractions was run on 4 to 20% Bio-Rad SDS–polyacrylamide gel electrophoresis gels and transferred to polyvinylidene difluoride membranes. After blocking with 5% nonfat dry milk in tris-buffered saline containing 0.1% Tween 20 for 1 hour at room temperature, membranes were incubated with rabbit anti-PBX1 polyclonal antibody (Cell Signaling) or rabbit anti-RTKN antibody (Abcam) overnight at 4°C. Membranes were then washed and incubated with horseradish-conjugated IgG secondary antibody (Cell Signaling). Immunoblots were developed with Western enhanced chemiluminesence substrate (Cell Signaling). Bound antibodies were removed with the Restore Western Stripping Buffer (Thermo Fisher Scientific), and then membranes were incubated with mouse anti–β-actin antibody (Cell Signaling) to normalize protein content.

Statistical analysis

Differences between groups were evaluated by two-tailed statistics: unpaired *t* tests and one-way analysis of variance (ANOVA) with Dunnett's multiple comparisons tests when more than two groups were compared. Nonparametric tests were used when the data were not normally distributed. Two-way ANOVA was used for time-course experiments. Unless specified, graphs show means and SDs of the mean. $*P < 0.05$, $**P < 0.01$, $***P < 0.001$, and $****P < 0.0001$.

Supplementary Materials

This PDF file includes:

Figs. S1 to S11
Tables S1 and S2

REFERENCES AND NOTES

1. S. Z. Josefowicz, L. F. Lu, A. Y. Rudensky, Regulatory T cells: Mechanisms of differentiation and function. *Annu. Rev. Immunol.* **30**, 531–564 (2012).

2. K. Wing, S. Sakaguchi, Regulatory T cells exert checks and balances on self tolerance and autoimmunity. *Nat. Immunol.* **11**, 7–13 (2010).
3. M. S. Jordan, A. Boesteanu, A. J. Reed, A. L. Petrone, A. E. Holenbeck, M. A. Lerman, A. Naji, A. J. Caton, Thymic selection of $CD4^+CD25^+$ regulatory T cells induced by an agonist self-peptide. *Nat. Immunol.* **2**, 301–306 (2001).
4. L. Morales-Nebreda, F. S. McLafferty, B. D. Singer, DNA methylation as a transcriptional regulator of the immune system. *Transl. Res.* **204**, 1–18 (2019).
5. N. Ohkura, M. Hamaguchi, H. Morikawa, K. Sugimura, A. Tanaka, Y. Ito, M. Osaki, Y. Tanaka, R. Yamashita, N. Nakano, J. Huehn, H. J. Fehling, T. Sparwasser, K. Nakai, S. Sakaguchi, T cell receptor stimulation-induced epigenetic changes and Foxp3 expression are independent and complementary events required for Treg cell development. *Immunity* **37**, 785–799 (2012).
6. W. Li, C. Deng, H. Yang, G. Wang, The regulatory T cell in active systemic lupus erythematosus patients: A systemic review and meta-analysis. *Front. Immunol.* **10**, 159 (2019).
7. K. Ohl, K. Tenbrock, Regulatory T cells in systemic lupus erythematosus. *Eur. J. Immunol.* **45**, 344–355 (2015).
8. T. Roach, L. Morel, Genetic variations controlling regulatory T cell development and activity in mouse models of lupus-like autoimmunity. *Front. Immunol.* **13**, 887489 (2022).
9. L. Chen, D. L. Morris, T. J. Vyse, Genetic advances in systemic lupus erythematosus: An update. *Curr. Opin. Rheumatol.* **29**, 423–433 (2017).
10. L. Morel, Mapping lupus susceptibility genes in the NZM2410 mouse model. *Adv. Immunol.* **115**, 113–139 (2012).
11. C. M. Cuda, S. Wan, E. S. Sobel, B. P. Croker, L. Morel, Murine lupus susceptibility locus Sle1a controls regulatory T cell number and function through multiple mechanisms. *J. Immunol.* **179**, 7439–7447 (2007).
12. C. M. Cuda, L. Zeumer, E. S. Sobel, B. P. Croker, L. Morel, Murine lupus susceptibility locus Sle1a requires the expression of two sub-loci to induce inflammatory T cells. *Genes Immun.* **11**, 542–553 (2010).
13. C. M. Cuda, S. Li, S. Liang, Y. Yin, H. H. S. K. Potula, Z. Xu, M. Sengupta, Y. Chen, E. Butfiloski, H. Baker, L. J. Chang, I. Dozmorov, E. S. Sobel, L. Morel, Pre-B cell leukemia homeobox 1 is associated with lupus susceptibility in mice and humans. *J. Immunol.* **188**, 604–614 (2012).
14. A. Laurent, R. Bihan, F. Omilli, S. Deschamps, I. Pellerin, PBX proteins: Much more than Hox cofactors. *Int. J. Dev. Biol.* **52**, 9–20 (2008).
15. C. G. Sagerstrom, PbX marks the spot. *Dev. Cell* **6**, 737–738 (2004).
16. F. Ficara, L. Crisafulli, C. Lin, M. Iwasaki, K. S. Smith, L. Zammataro, M. L. Cleary, Pbx1 restrains myeloid maturation while preserving lymphoid potential in hematopoietic progenitors. *J. Cell Sci.* **126**, 3181–3191 (2013).
17. F. Ficara, M. J. Murphy, M. Lin, M. L. Cleary, Pbx1 regulates self-renewal of long-term hematopoietic stem cells by maintaining their quiescence. *Cell Stem Cell* **2**, 484–496 (2008).
18. M. Sanyal, J. W. Tung, H. Karsunky, H. Zeng, L. Selleri, I. L. Weissman, L. A. Herzenberg, M. L. Cleary, B-cell development fails in the absence of the Pbx1 proto-oncogene. *Blood* **109**, 4191–4199 (2007).
19. S. Gu, J. Zhang, X. Han, H. Ding, C. Yao, Z. Ye, Z. Yin, G. Hou, Y. Jiang, J. Qian, H. Zhou, Q. Guo, S. Chen, D. Dai, N. Shen, Involvement of transcriptional factor Pbx1 in Peripheral B cell homeostasis to constrain lupus autoimmunity. *Arthritis Rheumatol. 75*, 1381–1394 (2023).
20. D. Penkov, M. Palazzolo, A. Mondino, F. Blasi, Cytosolic sequestration of Prep1 influences early stages of T cell development. *PLOS ONE* **3**, e2424 (2008).
21. M. Sengupta, S. Liang, H. H. Potula, L. J. Chang, L. Morel, The SLE-associated Pbx1-d isoform acts as a dominant-negative transcriptional regulator. *Genes Immun.* **13**, 653–657 (2012).
22. S. Lu, L. Zeumer, H. Sorensen, H. Yang, Y. Ng, F. Yu, A. Riva, B. Croker, S. Wallet, L. Morel, The murine Pbx1-d lupus susceptibility allele accelerates mesenchymal stem cell differentiation and impairs their immunosuppressive function. *J. Immunol.* **194**, 43–55 (2015).
23. E. S. Sobel, T. M. Brusko, E. J. Butfiloski, W. Hou, S. Li, C. M. Cuda, A. N. Abid, W. H. Reeves, L. Morel, Defective response of $CD4^+$ T cells to retinoic acid and TGFβ in systemic lupus erythematosus. *Arthritis Res. Ther.* **13**, R106 (2011).
24. S. C. Choi, T. E. Hutchinson, A. A. Titov, H. R. Seay, S. Li, T. M. Brusko, B. P. Croker, S. Salek-Ardakani, L. Morel, The lupus susceptibility gene Pbx1 regulates the balance between follicular helper T cell and regulatory T cell differentiation. *J. Immunol.* **197**, 458–469 (2016).
25. Y. X. Liao, J. M. Zeng, J. J. Zhou, G. H. Yang, K. Ding, X. J. Zhang, Silencing of RTKN2 by siRNA suppresses proliferation, and induces G1 arrest and apoptosis in human bladder cancer cells. *Mol. Med. Rep.* **13**, 4872–4878 (2016).
26. E. K. Wakeland, A. E. Wandstrat, K. Liu, L. Morel, Genetic dissection of systemic lupus erythematosus. *Curr. Opin. Immunol.* **11**, 701–707 (1999).
27. A. M. Thornton, P. E. Korty, D. Q. Tran, E. A. Wohlfert, P. E. Murray, Y. Belkaid, E. M. Shevach, Expression of Helios, an Ikaros transcription factor family member, differentiates thymic-derived from peripherally induced $Foxp3^+$ T regulatory cells. *J. Immunol.* **184**, 3433–3441 (2010).
28. C. H. Plunkett, C. R. Nagler, The influence of the microbiome on allergic sensitization to food. *J. Immunol.* **198**, 581–589 (2017).
29. T. Roach, Y. P. Park, S.-C. Choi, L. Morel, Regulation of the STAT3 pathway by lupus susceptibility gene Pbx1 in T cells. *Mol. Immunol.* **165**, 1–10 (2024).
30. J. Shimizu, S. Yamazaki, T. Takahashi, Y. Ishida, S. Sakaguchi, Stimulation of $CD25^+CD4^+$ regulatory T cells through GITR breaks immunological self-tolerance. *Nat. Immunol.* **3**, 135–142 (2002).
31. S. Deaglio, K. M. Dwyer, W. Gao, D. Friedman, A. Usheva, A. Erat, J. F. Chen, K. Enjyoji, J. Linden, M. Oukka, V. K. Kuchroo, T. B. Strom, S. C. Robson, Adenosine generation catalyzed by CD39 and CD73 expressed on regulatory T cells mediates immune suppression. *J. Exp. Med.* **204**, 1257–1265 (2007).
32. B. S. Kim, H. Lu, K. Ichiyama, X. Chen, Y. B. Zhang, N. A. Mistry, K. Tanaka, Y. H. Lee, R. Nurieva, L. Zhang, X. Yang, Y. Chung, W. Jin, S. H. Chang, C. Dong, Generation of $ROR\gamma t^+$ antigen-specific T regulatory 17 cells from $Foxp3^+$ precursors in autoimmunity. *Cell Rep.* **21**, 195–207 (2017).
33. D. Tischner, I. Gaggl, I. Peschel, M. Kaufmann, S. Tuzlak, M. Drach, N. Thuille, A. Villunger, G. Jan Wiegers, Defective cell death signalling along the Bcl-2 regulated apoptosis pathway compromises Treg cell development and limits their functionality in mice. *J. Autoimmun.* **38**, 59–69 (2012).
34. Y. Liu, T. Zhu, G. Cai, Y. Qin, W. Wang, G. Tang, D. Zhao, Q. Shen, Elevated circulating $CD4^+$ $ICOS^+$ $Foxp3^+$ T cells contribute to overproduction of IL-10 and are correlated with disease severity in patients with systemic lupus erythematosus. *Lupus* **20**, 620–627 (2011).
35. M. D. Vu, X. Xiao, W. Gao, N. Degauque, M. Chen, A. Kroemer, N. Killeen, N. Ishii, X. Chang Li, OX40 costimulation turns off $Foxp3^+$ Tregs. *Blood* **110**, 2501–2510 (2007).
36. A. M. Baru, A. Hartl, K. Lahl, J. K. Krishnaswamy, H. Fehrenbach, A. Ö. Yildirim, H. Garn, H. Renz, G. M. N. Behrens, T. Sparwasser, Selective depletion of $Foxp3^+$ Treg during sensitization phase aggravates experimental allergic airway inflammation. *Eur. J. Immunol.* **40**, 2259–2266 (2010).
37. X. Zhou, S. L. Bailey-Bucktrout, L. T. Jeker, C. Penaranda, M. Martínez-Llordella, M. Ashby, M. Nakayama, W. Rosenthal, J. A. Bluestone, Instability of the transcription factor Foxp3 leads to the generation of pathogenic memory T cells in vivo. *Nat. Immunol.* **10**, 1000–1007 (2009).
38. M. Yokogawa, M. Takaishi, K. Nakajima, R. Kamijima, C. Fujimoto, S. Kataoka, Y. Terada, S. Sano, Epicutaneous application of toll-like receptor 7 agonists leads to systemic autoimmunity in wild-type mice: A new model of systemic lupus erythematosus. *Arthritis Rheumatol.* **66**, 694–706 (2014).
39. Y. Xu, L. Zeumer, W. H. Reeves, L. Morel, Induced murine models of systemic lupus erythematosus. *Methods Mol. Biol.* **1134**, 103–130 (2014).
40. X. Liu, X. Chen, B. Zhong, A. Wang, X. Wang, F. Chu, R. I. Nurieva, X. Yan, P. Chen, L. G. van der Flier, H. Nakatsukasa, S. S. Neelapu, W. Chen, H. Clevers, Q. Tian, H. Qi, L. Wei, C. Dong, Transcription factor achaete-scute homologue 2 initiates follicular T-helper-cell development. *Nature* **507**, 513–518 (2014).
41. J. Choi, H. Diao, C. E. Faliti, J. Truong, M. Rossi, S. Bélanger, B. Yu, A. W. Goldrath, M. E. Pipkin, S. Crotty, Bcl-6 is the nexus transcription factor of T follicular helper cells via repressor-of-repressor circuits. *Nat. Immunol.* **21**, 777–789 (2020).
42. S. Reißig, Y. Tang, A. Nikolaev, K. Gerlach, C. Wolf, K. Davari, C. Gallus, J. Masri, I. A. Mufazalov, M. F. Neurath, F. T. Wunderlich, J. M. Schattenberg, P. R. Galle, B. Weigmann, A. Waisman, E. Glasmacher, N. Hövelmeyer, Elevated levels of Bcl-3 inhibits Treg development and function resulting in spontaneous colitis. *Nat. Commun.* **8**, 15069 (2017).
43. F. Renoux, M. Stellato, C. Haftmann, A. Vogetseder, R. Huang, A. Subramaniam, M. O. Becker, P. Blyszczuk, B. Becher, J. H. W. Distler, G. Kania, O. Boyman, O. Distler, The AP1 transcription factor Fosl2 promotes systemic autoimmunity and inflammation by repressing Treg development. *Cell Rep.* **31**, 107826 (2020).
44. S. Lee, K. Park, J. Kim, H. Min, R. H. Seong, Foxp3 expression in induced regulatory T cells is stabilized by C/EBP in inflammatory environments. *EMBO Rep.* **19**, e45995 (2018).
45. I. Y. Hwang, C. Park, K. Harrison, C. Boularan, C. Galés, J. H. Kehrl, An essential role for RGS protein/$G\alpha_{i2}$ interactions in B lymphocyte-directed cell migration and trafficking. *J. Immunol.* **194**, 2128–2139 (2015).
46. T. Alissafi, L. Kalafati, M. Lazari, A. Filia, I. Kloukina, M. Manifava, J. H. Lim, V. I. Alexaki, N. T. Ktistakis, T. Doskas, G. A. Garinis, T. Chavakis, D. T. Boumpas, P. Verginis, Mitochondrial oxidative damage underlies regulatory T cell defects in autoimmunity. *Cell Metab.* **32**, 591–604.e7 (2020).
47. Z. W. Lai, I. Marchena-Mendez, A. Perl, Oxidative stress and Treg depletion in lupus patients with anti-phospholipid syndrome. *Clin. Immunol.* **158**, 148–152 (2015).
48. M. Umeda, T. Koga, K. Ichinose, T. Igawa, T. Sato, A. Takatani, T. Shimizu, S. Fukui, A. Nishino, Y. Horai, Y. Hirai, S. Y. Kawashiri, N. Iwamoto, T. Aramaki, M. Tamai, H. Nakamura, K. Yamamoto, N. Abiru, T. Origuchi, Y. Ueki, A. Kawakami, $CD4^+$ $CD52^{lo}$ T-cell expression contributes to the development of systemic lupus erythematosus. *Clin. Immunol.* **187**, 50–57 (2018).
49. H. Zhang, A. Madi, N. Yosef, N. Chihara, A. Awasthi, C. Pot, C. Lambden, A. Srivastava, P. R. Burkett, J. Nyman, E. Christian, Y. Etminan, A. Lee, H. Stroh, J. Xia, K. Karwacz,

P. I. Thakore, N. Acharya, A. Schnell, C. Wang, L. Apetoh, O. Rozenblatt-Rosen, A. C. Anderson, A. Regev, V. K. Kuchroo, An IL-27-driven transcriptional network identifies regulators of IL-10 expression across T helper cell subsets. *Cell Rep.* **33**, 108433 (2020).
50. E. Y. Chung, J. Liu, Y. Homma, Y. Zhang, A. Brendolan, M. Saggese, J. Han, R. Silverstein, L. Selleri, X. Ma, Interleukin-10 expression in macrophages during phagocytosis of apoptotic cells is mediated by homeodomain proteins Pbx1 and Prep-1. *Immunity* **27**, 952–964 (2007).
51. S. Biswas, K. Bieber, R. A. Manz, IL-10 revisited in systemic lupus erythematosus. *Front. Immunol.* **13**, 970906 (2022).
52. X. Wang, L. Zhang, W. Wang, Y. Wang, Y. Chen, R. Xie, X. Li, Y. Wang, Rhotekin 2 silencing inhibits proliferation and induces apoptosis in human osteosarcoma cells. *Biosci. Rep.* **38**, bsr20181384 (2018).
53. A. Suarez-Fueyo, S. J. Bradley, G. C. Tsokos, T cells in systemic lupus erythematosus. *Curr. Opin. Immunol.* **43**, 32–38 (2016).
54. L. S. K. Walker, The link between circulating follicular helper T cells and autoimmunity. *Nat. Rev. Immunol.* **22**, 567–575 (2022).
55. M. Dall'Era, M. L. Pauli, K. Remedios, K. Taravati, P. M. Sandova, A. L. Putnam, A. Lares, A. Haemel, Q. Tang, M. Hellerstein, M. Fitch, J. McNamara, B. Welch, J. A. Bluestone, D. Wofsy, M. D. Rosenblum, the Autoimmunity Centers of Excellence, Adoptive Treg cell therapy in a patient with systemic lupus erythematosus. *Arthritis Rheumatol.* **71**, 431–440 (2019).
56. R. Akbarzadeh, G. Riemekasten, J. Y. Humrich, Low-dose interleukin-2 therapy: A promising targeted therapeutic approach for systemic lupus erythematosus. *Curr. Opin. Rheumatol.* **35**, 98–106 (2023).
57. S. Wan, C. Xia, L. Morel, IL-6 produced by dendritic cells from lupus-prone mice inhibits $CD4^+CD25^+$ T cell regulatory functions. *J. Immunol.* **178**, 271–279 (2007).
58. S. Srivastava, M. A. Koch, M. Pepper, D. J. Campbell, Type I interferons directly inhibit regulatory T cells to allow optimal antiviral T cell responses during acute LCMV infection. *J. Exp. Med.* **211**, 961–974 (2014).
59. L. Morel, K. R. Blenman, B. P. Croker, E. K. Wakeland, The major murine systemic lupus erythematosus susceptibility locus, Sle1, is a cluster of functionally related genes. *Proc. Natl. Acad. Sci. U.S.A.* **98**, 1787–1792 (2001).
60. E. S. Sobel, M. Satoh, W. F. Chen, E. K. Wakeland, L. Morel, The major murine systemic lupus erythematosus susceptibility locus *Sle1* results in abnormal functions of both B and T cells. *J. Immunol.* **169**, 2694–2700 (2002).
61. D. J. Perry, Y. Yin, T. Telarico, H. V. Baker, I. Dozmorov, A. Perl, L. Morel, Murine lupus susceptibility locus *Sle1c2* mediates $CD4^+$ T cell activation and maps to estrogen-related receptor γ. *J. Immunol.* **189**, 793–803 (2012).
62. W. Li, M. Gong, Y. P. Park, A. S. Elshikha, S. C. Choi, J. Brown, N. Kanda, W. I. Yeh, L. Peters, A. A. Titov, X. Teng, T. M. Brusko, L. Morel, Lupus susceptibility gene Esrrg modulates regulatory T cells through mitochondrial metabolism. *JCI Insight* **6**, e143540 (2021).
63. Y. P. Park, T. Roach, S. Soh, L. Zeumer-Spataro, S. C. Choi, D. A. Ostrov, Y. Yang, L. Morel, Molecular mechanisms of lupus susceptibility allele PBX1D. *J. Immunol.* **211**, 727–734 (2023).
64. A. L. Bishop, A. Hall, Rho GTPases and their effector proteins. *Biochem. J.* **348** (Pt. 2), 241–255 (2000).
65. F. M. Collier, C. C. Gregorio-King, T. J. Gough, C. D. Talbot, K. Walder, M. A. Kirkland, Identification and characterization of a lymphocytic Rho-GTPase effector: Rhotekin-2. *Biochem. Biophys. Res. Commun.* **324**, 1360–1369 (2004).
66. R. Bhairavabhotla, Y. C. Kim, D. D. Glass, T. M. Escobar, M. C. Patel, R. Zahr, C. K. Nguyen, G. K. Kilaru, S. A. Muljo, E. M. Shevach, Transcriptome profiling of human $FoxP3^+$ regulatory T cells. *Hum. Immunol.* **77**, 201–213 (2016).
67. F. M. Collier, A. Loving, A. J. Baker, J. McLeod, K. Walder, M. A. Kirkland, RTKN2 induces NF-KappaB dependent resistance to intrinsic apoptosis in HEK cells and regulates BCL-2 genes in human $CD4^+$ lymphocytes. *J Cell Death* **2**, 9–23 (2009).
68. K. Myouzen, Y. Kochi, Y. Okada, C. Terao, A. Suzuki, K. Ikari, T. Tsunoda, A. Takahashi, M. Kubo, A. Taniguchi, F. Matsuda, K. Ohmura, S. Momohara, T. Mimori, H. Yamanaka, N. Kamatani, R. Yamada, Y. Nakamura, K. Yamamoto, Functional variants in NFKBIE and RTKN2 involved in activation of the NF-κB pathway are associated with rheumatoid arthritis in Japanese. *PLOS Genet.* **8**, e1002949 (2012).
69. N. Hovelmeyer, M. Schmidt-Supprian, C. Ohnmacht, NF-κB in control of regulatory T cell development, identity, and function. *J. Mol. Med. (Berl)* **100**, 985–995 (2022).
70. H. Oh, Y. Grinberg-Bleyer, W. Liao, D. Maloney, P. Wang, Z. Wu, J. Wang, D. M. Bhatt, N. Heise, R. M. Schmid, M. S. Hayden, U. Klein, R. Rabadan, S. Ghosh, An NF-κB transcription-factor-dependent lineage-specific transcriptional program promotes regulatory T cell identity and function. *Immunity* **47**, 450–465.e5 (2017).
71. N. Messina, T. Fulford, L. O'Reilly, W. X. Loh, J. M. Motyer, D. Ellis, C. McLean, H. Naeem, A. Lin, R. Gugasyan, R. M. Slattery, R. J. Grumont, S. Gerondakis, The NF-κB transcription factor RelA is required for the tolerogenic function of $Foxp3^+$ regulatory T cells. *J. Autoimmun.* **70**, 52–62 (2016).
72. X. Pang, R. Li, D. Shi, X. Pan, C. Ma, G. Zhang, C. Mu, W. Chen, Knockdown of Rhotekin 2 expression suppresses proliferation and induces apoptosis in colon cancer cells. *Oncol. Lett.* **14**, 8028–8034 (2017).
73. H. G. Zhao, J. J. Yin, X. Chen, J. Wu, W. Wang, L. W. Tang, RTKN2 enhances radioresistance in gastric cancer through regulating the Wnt/β-Catenin signalling pathway. *Folia Biol.* **68**, 33–39 (2022).
74. J. van Loosdregt, V. Fleskens, M. M. Tiemessen, M. Mokry, R. van Boxtel, J. Meerding, C. E. G. M. Pals, D. Kurek, M. R. M. Baert, E. M. Delemarre, A. Gröne, M. J. A. G. Koerkamp, A. J. A. M. Sijts, E. E. S. Nieuwenhuis, M. M. Maurice, J. H. van Es, D. ten Berge, F. C. Holstege, F. J. T. Staal, D. M. W. Zaiss, B. J. Prakken, P. J. Coffer, Canonical Wnt signaling negatively modulates regulatory T cell function. *Immunity* **39**, 298–310 (2013).
75. X. Xu, Y. Zhou, B. Fu, J. Zhang, Z. Dong, X. Zhang, N. Shen, R. Sun, Z. Tian, H. Wei, PBX1 promotes development of natural killer cells by binding directly to the *Nfil3* promoter. *FASEB J.* **34**, 6479–6492 (2020).
76. H. S. Kim, H. Sohn, S. W. Jang, G. R. Lee, The transcription factor NFIL3 controls regulatory T-cell function and stability. *Exp. Mol. Med.* **51**, 1–15 (2019).
77. L. Morel, B. P. Croker, K. R. Blenman, C. Mohan, G. Huang, G. Gilkeson, E. K. Wakeland, Genetic reconstitution of systemic lupus erythematosus immunopathology with polycongenic murine strains. *Proc. Natl. Acad. Sci. U.S.A.* **97**, 6670–6675 (2000).
78. S. C. Choi, A. A. Titov, G. Abboud, H. R. Seay, T. M. Brusko, D. C. Roopenian, S. Salek-Ardakani, L. Morel, Inhibition of glucose metabolism selectively targets autoreactive follicular helper T cells. *Nat. Commun.* **9**, 4369 (2018).
79. C. Mohan, E. Alas, L. Morel, P. Yang, E. K. Wakeland, Genetic dissection of SLE pathogenesis. Sle1 on murine chromosome 1 leads to a selective loss of tolerance to H2A/H2B/DNA subnucleosomes. *J. Clin. Invest.* **101**, 1362–1372 (1998).
80. Y. Ge, M. Zadeh, M. Mohamadzadeh, Vitamin B12 coordinates ileal epithelial cell and microbiota functions to resist Salmonella infection in mice. *J. Exp. Med.* **219**, e20220057 (2022).

Acknowledgments: We thank L. Zeumer-Spataro, N. Kanda, the staff from the UF Lupus Clinic for technical assistance, and the staff from the Flow Cytometry Shared Resource at UTHSA. **Funding:** This study was supported by a grant from the National Institutes of Health (R01 AI045050) to L.M. The Flow Cytometry Shared Resource at UTHSA is supported by a grant from the National Cancer Institute (P30CA054174) to the Mays Cancer Center, a grant from the Cancer Prevention and Research Institute of Texas (CPRIT) (RP210126) and a grant from the National Institutes of Health (S10OD030432), both awarded to M. Berton, core director. **Author contributions:** Conceptualization: S.-C.C., Y.P.P., and L.Mo. Methodology: S.-C.C., Y.G., M.M., and L.Mo. Investigation: S.-C.C., Y.P.P., T.R., D.J., A.F., M.Z., Y.G., E.S.S., and L. Ma. Supervision: M.M. and L.Mo. Writing—original draft: S.-C.C. and L.Mo. Writing—review and editing: T.R., L. Ma, and M.M. **Competing interests:** The authors declare that they have no competing interests. **Data and materials availability:** All data needed to evaluate the conclusions in the paper are present in the paper and/or the Supplementary Materials. The transcriptomic raw FastQ files have been submitted to the Sequence Read Archive (SRA) and are available under the accession number PRJNA961793 at the NCBI BioProject.

Submitted 25 April 2023
Accepted 22 February 2024
Published 27 March 2024
10.1126/sciadv.adi4310